SLOW MOVING AND LATENT SYSTEMIC RISK: EVIDENCE FROM AGRICULTURAL COMMODITIES

Polina Bulavko[1]
DRM-Finance, PSL Research University Paris-Dauphine; MATS; FiME

Delphine Lautier[1]
DRM-Finance, PSL Research University Paris-Dauphine; MATS; FiME

Julien Ling[1]
Collège de France; Institut Louis Bachelier; MATS; FiME

April 29, 2026

This is a preliminary draft. Do not circulate.

Does the temporal structure of information arrival - whether abrupt or gradual - determine the topology of financial networks? We distinguish between "fast-breaking" financial surprises, showing that they fragment networks or weaken linkages, and a "slow-building" physical shock, which allows for latency in information aggregation and leads to increased clustering and stronger connections. We reconstruct time-varying networks of agricultural futures markets using daily returns for ten commodities over the period 2004–2024, applying Sparse VAR Network Estimation (`nets`). This enables the simultaneous estimation of contemporaneous and predictive networks, where we find that the former are dense, with grain and soft commodities forming distinct clusters, and the latter are relatively sparse, with central nodes such as soybeans and corn acting as shock transmitters. Dynamic network analysis reveals that fast market shocks (e.g., the 2008 Lehman Brothers collapse and the 2020 WTI crash) trigger immediate spikes in the strength of predictive spillovers and a decline in contemporaneous dependence. To study slow shocks, we implement a novel endogenous network Difference-in-Differences design on dynamic graph intensities, exploiting the 2012 U.S. Midwest drought as a natural experiment. In striking contrast to financial shocks, we find that this gradual physical shock induces an increase in the strength of contemporaneous linkages around the core grain complex. This "clustering" phenomenon reveals a latent form of systemic risk: during slow shocks characterized by a series of uncertainty-resolving events, network reorganization may override idiosyncratic fundamentals, likely causing standard diversification strategies to fail.

JEL: G01, G13, Q02, Q14, Q42, Q54, C32

Keywords: Systemic risk; sparse VAR; causal inference; difference-in-differences; futures markets; agricultural commodities; graph theory

---

Acknowledgements. We warmly thank Franck Raynaud (University of Geneva) for his valuable comments on the methodology and paper design. We thank Michel Robe (University of Richmond) for his in-depth insights on agricultural commodities. We thank Bertrand Villeneuve (Paris-Dauphine) and other participants for the valuable feedback during MATS Summer School 2025 in Aussois. We thank Camille Ait-Youcef (Nantes University) her positive comments during the commodity workshop 2025 in Nantes, and all the participants. We also thank Amedeo Andriollo (Paris-Dauphine) for his insights on the econometric empirical design. Finally, we are grateful to MATS project, and all the participants of the MATS Seminar 2024 in Paris.

[*]Emails: polina.bulavko@dauphine.eu; delphine.lautier@dauphine.psl.eu; julien.ling@institutlouisbachelier.org

1. Introduction

Do extreme weather events that affect some agricultural markets propagate to others? Can we fear that, due to the financialization of commodities, such events might reach financial assets? In this paper, we investigate whether an extreme event that has impacted two main cereals in the United States, the 2012 drought, has such an impact. This event is especially interesting because it is a «slow building» shock, to be distinguished with «fast breaking» financial surprises.

Systemic risk arises from the network of financial interdependencies, through which shocks propagate and amplify (Acemoglu, Ozdaglar, and Tahbaz-Salehi 2015; Elliott, Golub, and Jackson 2014). Yet, the financial contagion literature typically models shocks as discrete events and focuses on the resulting transmission topology. This framework is less well suited to shocks whose underlying fundamentals are revealed gradually and lack a well-defined event time. We propose that the speed at which uncertainty resolves shapes how financial networks reorganize under stress, leading to either stronger links/clustering or weaker links/fragmentation.[1] Specifically, we distinguish between shocks that arrive as instantaneous surprises and those that unfold through sequential information updates, and show that this temporal structure of information can be a determinant of network reorganization, with distinct implications for systemic risk.

Fast shocks (e.g., the Lehman Brothers collapse on September 15, 2008, the 2020 WTI crash, and the Russian invasion on February 24, 2022) arrive as discrete, instantaneous events often. Although these events often represent the culmination of accumulated structural fragility or bubble bursts, their defining feature is that the lion's share of fundamental information is realized abruptly. These shocks force speculators and arbitrageurs to unwind positions under liquidity stress (Büyükşahin and Robe 2024; Mitchell, Lasse H. Pedersen, and Pulvino 2007; I.-H. Cheng and Xiong 2014). As Duffie (2010) establishes, immediate risk-bearing capacity is severely constrained by search frictions and inattention, hence in times of stress, hedgers are not spared either. This might result in a temporary rise in predictive spillovers and a weakening/fragmentation of cross-market dependence.

[1] In graph-theoretic terms, stronger or weaker links refer to changes in edge weights, such as higher or lower correlations between nodes. Clustering denotes greater local interconnectedness among nodes, and fragmentation refers to a loss of connectivity, whereby links disappear and the network may break into disconnected components. A network is dense if it has a high number of edges relative to the number of possible links, and sparse if it has relatively few.

Our first contribution is to characterize slow shocks (e.g., droughts, gradual policy changes, or sequential geopolitical sanctions) as processes in which information is revealed incrementally. This extended resolution horizon allows agents to aggregate information across assets and gradually rebalance hedging positions. For example, Letta, Montalbano, and Pierre (2022) document that agricultural traders anticipate more than 80% of a supply shock before the physical harvest damage materializes. These mechanisms lead to greater market integration and clustering, yet remain largely invisible to conventional stress tests for systemic risk (Lautier and Raynaud 2012; Lautier, Ling, and Raynaud 2015). This form of structural reorganization may be obscured by macroeconomic noise or misattributed to common factors. However, it represents a distinct and latent form of systemic risk, characterized by a gradual strengthening (or clustering) of connections, in contrast to the abrupt and liquidity-driven weakening (or fragmentation) observed during fast financial shocks. Our main contribution is to provide both an empirical setting and a methodological framework to identify and measure the effects arising from slow shocks.

Agricultural markets provide a natural setting to study the differential impact of fast and slow shocks, as they exhibit a form of "dual exposure": spot prices respond directly to physical production outcomes driven by meteorological conditions, while futures prices embed global financial linkages through hedging, index investment, and algorithmic trading (I.-H. Cheng and Xiong 2014; Sanders, S. H. Irwin, and Merrin 2010; Aulerich, S. H. Irwin, and Garcia 2014). As a result, these markets are exposed to fast financial shocks such as the Lehman, while also exhibiting a distinct temporal structure that characterizes slow shocks. The uncertainty surrounding weather-induced supply disruptions is bounded by the biological growing season, and information about yield deterioration is revealed sequentially through periodic USDA crop condition reports.[2] Consistent with this mechanism, A. N. Cao and Robe (2022) show that while agricultural volatility typically tracks global financial sentiment (VIX), it decouples during USDA announcement days, indicating that physical information drives distinct pricing dynamics. We exploit this gradual information revelation window, anchored in meteorological conditions and the crop cycle, which defines the period over which drought-related information is incorporated into prices. We then develop an empirical framework that disentangles the effects of the slow shock from other shocks affecting commodity prices during this period.

[2]Agricultural crops are continuously monitored via weather forecasts, satellite imagery, and weekly USDA reports. As a result, even rapid biophysical deterioration is incorporated into prices gradually, as a sequence of information updates rather than a single discrete shock (Letta, Montalbano, and Pierre 2022).

Before analyzing slow shocks, it is necessary to understand how agricultural markets are interconnected, and here lies our empirical contribution. We rely on graph theory because it synthesizes high-dimensional price systems, allowing us to extract metrics - such as network intensity and node centrality - that reveal more about systemic vulnerability than conventional analyses. We begin by providing, to the best of our knowledge, the most comprehensive characterization to date of both contemporaneous and predictive network structures in agricultural futures, covering ten commodities over the period 2004–2024. The contemporaneous network captures the degree of market integration, while the predictive network provides insight into shock propagation. To estimate these networks, we employ the sparse vector autoregressive (VAR) framework (`nets`) of Barigozzi and Brownlees (2019) using daily futures returns. Using LASSO regularization, this approach simultaneously constructs time-varying networks that capture both contemporaneous dependencies (via partial correlations) and predictive relationships separately.

Topology of the graph reveals that, in the dense contemporaneous network, agricultural commodities organize into clusters of grains (core, soybeans - soybean oil - soybean meal and corn - wheat clusters) and softs (peripheral, cocoa US - cocoa UK, and coffee - cotton - sugar). This core-periphery topology reflects the high degree of substitutability among grains relative to softs. The predictive network is relatively sparse, consistent with the high degree of informational efficiency in financialized commodity markets. This is consistent with Adjemian (2012), who shows that scheduled USDA announcements trigger immediate price discovery and volatility resolution. Grains emerge as primary transmitters of shocks while softs act predominantly as receivers. To further characterize this structure, we adapt the total communicability centrality measure to our setting and show that soybeans, soybean oil, soybean meal, and corn are the most central commodities. This pattern raises concerns about systemic risk, as Paris (2018) and S. H. Kang, Tiwari, et al. (2019) show that the grain core serves as a critical bridge to broader energy and livestock markets via biofuel and feed demand. We also find that connectivity levels (network intensity) fluctuate over time, being higher in 2008-2010 (commodity prices boom), 2017-2018, and 2021-2024 (post-pandemic inflationary environment).

This baseline framework can capture the response of network structure to stress: fast financial surprises (e.g., the Lehman Brothers collapse, WTI turning negative, JP Morgan quitting physical commodity trading etc.) trigger immediate spikes in predictive spillovers and a decline in strength of contemporaneous dependence. However, it does

not detect a comparable response to the 2012 drought. This absence of a detectable response reflects a fundamental identification challenge. Unlike fast financial shocks, slow-moving physical shocks unfold gradually and do not have a well-defined event time. Moreover, agricultural networks evolve continuously due to endogenous factors such as substitution patterns, seasonality, and financialization trends. As a result, distinguishing shock-induced structural clustering from normal correlation drift requires a setting with strictly exogenous shocks and clearly defined timing variation.

This paper thus exploits the 2012 U.S. drought - one of the most severe agricultural supply shocks in recent decades[3] - as a natural experiment in agricultural commodity futures markets. To test for the causal impact of a physical shock on network topology, we implement a novel experimental difference-in-differences (DiD) design. This design avoids the simultaneity bias that would arise if treatment assignment relied on contemporaneous network adjustments. Instead, treatment status is assigned based solely on ex-ante network proximity. Specifically, for each year between 2006 and 2023, we split commodities into "highly exposed" or "baseline" based on their pre-shock conditional dependence on an anchor basket centered on grains directly affected by the drought. We then test whether the difference in contemporaneous connectivity between highly and weakly exposed commodities changes during the drought window relative to the pre-period. Estimation proceeds using the group-time average treatment effect framework of Callaway and Sant'Anna (2021). This design aligns with recent advances in causal inference under network interference (Jetsupphasuk, D. Li, and Hudgens 2025) and cleanly resolves the endogeneity arising from simultaneous network evolution.

Empirically, 2012 stands out clearly in the data. Across 21 alternative specifications[4] , the estimated effects in 2012 are consistently positive (>0) and statistically significant. In contrast, other years exhibit substantially weaker and less stable patterns. These results indicate that the 2012 drought is associated with a robust and interpretable reorganization of contemporaneous conditional dependence in the agricultural network, characterized by a strengthening of existing connections and weaking or fragmentation of ex-ante weaker links, i.e. clustering. Overall, we document that while "fast-breaking" financial

[3]For example, during the 2012 U.S. drought, as documented in USDA crop progress reports, the growing season began with manageable expectations; for June 10, 2012, 54% of the corn crop was rated "Good" and 12% "Excellent" (USDA, NASS 2012a). However, as the drought intensified during the critical pollination window, asset quality collapsed. By the week ending July 22, 2012, only 23% of the crop remained "Good" with a mere 3% rated "Excellent" (USDA, NASS 2012b).

[4]As many to ensure robustness.

surprises trigger an immediate weakening of network interlinkages, the "slow-building" physical shock of the 2012 drought induces a structural densification and strengthening around the network core. Consequently, gradual physical stress overrides independent fundamentals, reducing the effectiveness of traditional diversification precisely when it is most needed. To capture this latent systemic risk, "slow shocks" require a fundamentally different identification strategy than fast financial surprises. Our dynamic, within-network difference-in-differences design provides such a framework.

The remainder of the paper is organized as follows. Section 2 reviews the related literature. Section 3 develops the conceptual framework. Section 4 describes the data, network construction using `nets`, and the difference-in-differences design. Section 5 presents the empirical results. Section 6 concludes.

2. Literature Review

This paper integrates four distinct branches of literature: systemic risk, commodity connectedness, impact of climate on commodities, limits to arbitrage, and network causal inference.

Systemic risk has been characterized along several dimensions. One view emphasizes disruptions to financial intermediation and real economic activity (Bisias et al. 2012; V. Acharya, Engle, and Richardson 2012). Another focuses on contagion through interconnected balance sheets and financial networks (Elliott, Golub, and Jackson 2014; Acemoglu, Ozdaglar, and Tahbaz-Salehi 2015). A third highlights amplification mechanisms such as liquidity spirals, deleveraging, and fire-sale externalities (Markus K. Brunnermeier and Lasse Heje Pedersen 2009; Duarte and Eisenbach 2021). Our paper relates most directly to the empirical strand that studies systemic risk through spillovers and connectedness, viewing shock transmission as an evolving network phenomenon observable in price returns, volatilities, and predictive dependencies. We thus define systemic risk as a shock that might have negative external effects on the financial system due to the interactions among financial (in our case derivatives) markets. Therefore, systemic risk is rising when financial markets are more interconnected, and climate risk is found to have a significant positive impact on connectivity in all market states (crisis and normal times).

Precisely, the propagation of systemic shocks is shaped by the economic frictions that constrain cross-market arbitrage. Existing literature provides both theoretical and empirically grounded mechanisms through which such frictions become binding during

crises. Markus K. Brunnermeier and Lasse Heje Pedersen (2009) establish the foundational link between funding liquidity and market liquidity, demonstrating that during crises, escalating margin requirements force constrained intermediaries to de-lever, triggering mutually reinforcing margin and loss spirals that abruptly dry up market liquidity. Within commodity markets specifically, V. V. Acharya, Lochstoer, and Ramadorai (2013) formalize how these limits to financial arbitrage generate limits to hedging for producers in the real economy. They document that the finite risk-bearing capacity of broker-dealers dictates the risk premium required to absorb producers' hedging pressure, meaning that speculator capital constraints directly affect equilibrium hedging costs and ultimately impact commodity supply and spot prices. When discrete financial distress materializes, these capital constraints bind abruptly. As I.-H. Cheng, Kirilenko, and Xiong (2015) demonstrate, spikes in global financial uncertainty force financial traders to aggressively reduce their net long positions, forcing them to transition from liquidity providers to liquidity demanders. This sudden unwinding generates "convective risk flows" that force commercial hedgers to absorb the displaced risk, temporarily dislocating futures prices from physical fundamentals.

Our paper contributes by showing that the topology of transmission is not the same when the shock is revealed gradually: abrupt shocks generate fragmentation and stronger predictive spillovers, whereas gradual shocks produce tighter contemporaneous clustering. In this sense, our results provide a possible network-level characterization of the frictional adjustment mechanisms emphasized in the existing literature. Regarding temporality, the inability of outside capital to instantaneously correct price dislocations is explained by the inherently "slow-moving" nature of arbitrage capital. Empirically, Mitchell, Lasse H. Pedersen, and Pulvino (2007) demonstrate that following severe capital shocks, market frictions and information barriers prevent immediate capital replenishment, allowing mispricing to persist for months. Theoretically, Duffie (2010) attributes this inertia to search frictions, institutional impediments, and investor inattention: because only a limited subset of capital is immediately available to absorb sudden supply or demand shocks on short notice, prices must initially overshoot to compensate available investors. This is followed by a gradual reversal as extended time horizons provide the necessary latency for new intermediaries to mobilize liquidity and systematically distribute the risk.

The global co-dependence of commodity markets is related to financialization of commodity markets that became the main driver of increasing interlinkages across different

commodity markets (Ekeland, Lautier, and Villeneuve 2019; Basak and Pavlova 2016). Existing evidence documents pronounced asymmetries in commodity spillovers, with certain sectors systematically acting as net transmitters while others predominantly absorb shocks (Xiao et al. 2020; S. H. Kang, McIver, and Yoon 2017). In particular, energy and metals tend to occupy central transmitting roles, whereas agricultural commodities are more often positioned as receivers, with stronger spillovers observed between energy and other sectors than between agriculture and metals (Shahzad et al. 2021). This asymmetry implies that the organization of agricultural markets is largely shaped by shocks originating in more central sectors, making their network structure particularly sensitive to external disturbances. In addition, Khalfaoui et al. (2021) specify that the transmission channels from energy to non-energy commodities can be production and logistics costs, supply shocks, speculative and herding behavior.

Bouri et al. (2021) find that volatility connectedness is stronger for energy and metals than for agricultural commodities. There is evidence that the complexity of the volatility between energy and agriculture increased because of the expansion of the ethanol market (Saghaian et al. 2018). S. H. Kang, Tiwari, et al. (2019) show that vegetable oils are the greatest contributors to price fluctuations of agricultural commodities and oil, and they are also the volatility transmitters. Paris (2018) shows evidence that agricultural commodity prices rise in the long-term because of the growing production of biofuels which increases the oil-price effect on the agricultural prices. The impact is transmittable within agricultural commodities through the substitution effect. This provides a view of agricultural commodities being seen as "energy commodities at the expense of their food purpose".

The increases in agricultural commodity prices that are caused by weather disruptions are found to worsen the economic activity especially in advanced countries despite the lower share of food in consumption baskets (De Winne and Peersman 2021). The impacts of climate shocks on commodity connectedness are well-documented but the evidences are mixed. Makkonen et al. (2021) show evidence of negative impact of temperature anomalies on the futures returns of ags in low quantiles and positive impact on the returns in high quantiles. Zhang et al. (2023) show that weather conditions affect commodity market interdependence more strongly in the long run than in the short run, with low temperature playing a key role in driving co-movement. One channel operates through energy markets: weather-induced disruptions in major producing regions such as Texas

can constrain oil and gas supply, with spillovers to agricultural and metal commodities via input costs and biofuel linkages. They further find that while global warming tends to weaken price linkages, short-run temperature anomalies can increase return spillovers by amplifying supply disruptions and energy demand. Y. Cao, S. Cheng, and X. Li (2024) find that bidirectional spillovers between oil and food markets is positive and asymmetric, and that temperature changes amplify the spillover effects.

Most of weather-price literature relies on reduced-form responses to contemporaneous weather variables or aggregate climate indicators. Such approaches are useful for identifying weather sensitivities, but they are less able to capture the full market impact of slow-moving climate events such as droughts. Climate shocks information arrival is assymetric, the price response is primarily based on expectations, and expectations are formed through satellite data forecasts, USDA reports, and information from actual fields. Inspired by storage theory, Letta, Montalbano, and Pierre (2022) exploit lags between weather shocks and supply shocks and find that drought significantly increases food prices before the harvest - meaning before an actual damage. This implies that markets update their beliefs and respond to expected supply shortfalls immediately. A. N. Cao and Robe (2022) show that while agricultural volatility typically tracks global financial sentiment (VIX), it decouples significantly during fundamental USDA announcement days, confirming that physical information drives distinct pricing dynamics. Adjemian (2012) demonstrates that scheduled USDA announcements trigger immediate price discovery and volatility resolution. Grains emerge as primary transmitters of shocks while softs act predominantly as receivers. Besides climate, Peng et al. (2021) document that soybean futures liquidity collapsed weeks before the 2020 financial crash, effectively signaling the impending demand shock from China before it registered in equity markets. Building on these insights, our empirical design treats drought as a gradual information process and constructs a testing framework that accounts for the sequential arrival of climate information rather than relying on contemporaneous weather realizations.

To empirically test for systemic risk, correlation and connectedness methods are widely explored. One of the first robust methodology using correlations is Minimum Spanning Tree presented in Lautier and Raynaud (2012) and originally developed by Mantegna (1999). The dynamic equicorrelation (DECO) approach (S. H. Kang, McIver, and Yoon 2017; Zhang et al. 2023) was developed by Engle and Kelly (2012) and allows to effectively capture the average pairwise correlation. More advanced approaches that go beyond

pairwise correlation are the CoVar approach (Adrian and Markus K Brunnermeier 2011), and the marginal expected shortfall (MES) (V. Acharya, Engle, and Richardson 2012). One of the most popular methodologies to study connectedness is the one of Diebold and Yilmaz (2012) and Diebold and Yilmaz (2014). The approach is "build from pieces of variance decompositions" that allows to define weighted and directed networks. Newer approaches related to connectedness include Bykhovskaya (2022) and Mlikota (2023). To isolate direct structural relationships from pervasive macroeconomic noise, researchers have advanced sparse Vector Autoregression (VAR) models. By penalizing indirect partial correlations, sparse VAR methodologies map both the contemporaneous and predictive topological footprint of high-dimensional time series (Barigozzi and Brownlees 2019); this methodolgy is used in this paper.

Estimating the reorganization of financial networks during shocks is possible with causal inference techniques.[1] Recent breakthroughs in causal inference have begun to formally address these complexities by adapting difference-in-differences (DiD) frameworks to environments with network interference and dynamic confounding. Jetsupphasuk, D. Li, and Hudgens (2025) extend the canonical DiD estimator to accommodate explicit network dependency, demonstrating that when treatments exhibit bipartite interference - where an intervention on one set of nodes alters the potential outcomes of interconnected neighboring nodes - consistent estimation requires conditioning on a precise, pre-determined network exposure mapping. To handle latent, time-varying confounds that frequently violate standard parallel trends in evolving systems, Arkhangelsky et al. (2021) introduce the synthetic difference-in-differences estimator, proving that reweighting unexposed units to match pre-intervention trajectories effectively absorbs interactive, unobserved unit and time factors. When these latent confounds induce heterogeneous pre-trends, Freyaldenhoven, Hansen, and Shapiro (2019) establish that causal identification can be restored by exploiting covariates affected by the latent confound but not the shock itself, while S. J. Lee and Wooldridge (2023) and Liu and Sun (2019) develop unit-specific transformations and robust asymptotic tests to correct for heterogeneous trend dynamics. Furthermore, Callaway and Sant'Anna (2021) and Roth et al. (2023) demonstrate that traditional two-way fixed effects regressions fail under heterogeneous and staggered shock propagation, formalizing instead the estimation of dynamic, group-time average treatment

[1] Most causal-inference work on networks has emerged outside finance, mainly in biostatistics, epidemiology, and public health

effects that rely strictly on clean, not-yet-treated comparison groups.

3. Economic Mechanisms

Information arrival speed and network reorganization We propose that shock transmission in financial networks depends on the speed of information arrival. We distinguish between slow-building shocks, which unfold through sequential updates and allow gradual belief revision, and fast-breaking shocks, which materialize abruptly and compress adjustment into short horizons. Agricultural futures markets provide a natural laboratory to study this distinction, as contracts are jointly exposed to physical production shocks and financial events.

Slow shocks - such as droughts - are characterized by sequential information release, heterogeneous private signals, and extended resolution horizons. Uncertainty resolves incrementally (e.g., through recurring USDA crop condition reports), inducing continuous updating of expectations about aggregate supply. Because directly exposed contracts incorporate dispersed field-level information, they become informationally central in price discovery (Vives 2008). The extended adjustment window allows economic mechanisms to operate gradually: commercial hedgers revise cross-commodity hedge ratios, spread traders adjust relative-value positions, and substitution relationships bind as relative prices move (I.-H. Cheng, Kirilenko, and Xiong 2015).

These features imply a specific network response. As the shock unfolds, contemporaneous partial correlations[1] between directly exposed contracts and their economically linked substitutes should increase, reflecting tighter conditional dependence driven by substitution and hedging adjustments. Because public information is rapidly incorporated within the trading day (Adjemian 2012; A. N. Cao and Robe 2022), persistent Granger predictive relations should remain limited in daily data. Importantly, those gradual effects build up and persist over the uncertainty resolution window.

Fast shocks arrive as discrete, publicly observed events that compress belief updating into a narrow time interval. Sudden volatility spikes and margin constraints force rapid position reductions, unwind cross-commodity spreads, and curtail arbitrage capital (Mitchell, Lasse H. Pedersen, and Pulvino 2007; Duffie 2010). Adjustment occurs through immediate hedge liquidation rather than gradual hedge reoptimization.

The predicted network response is that contemporaneous partial correlations decline

[1]Formal definitions of contemporaneous partial correlations and Granger predictive relations are provided in Section 4.3.

or remain muted as cross-market arbitrage relationships break down. Short-lived increases in Granger predictive links may emerge as information cascades across liquidity tiers, but these dislocations should mean-revert quickly as funding conditions stabilize.

Mechanisms of network responses We propose three complementary mechanisms through which slow shocks can generate structural clustering in futures networks consistent with the observed network responses. Each mechanism operates through informational or physical frictions and therefore requires an extended resolution horizon.

Agricultural futures markets constitute almost "closed" ecosystems[2] with rigid biological constraints and defined substitution linkages (e.g., the corn-soybean rotation or feed-grain substitution S. Lee (2025)), creating a controlled environment to isolate the structural channels of shock transmission. Furthermore, liquidity dynamics in these markets can serve as leading indicators for broader systemic stress; Peng et al. (2021) document that soybean futures liquidity collapsed weeks before the 2020 financial crash, effectively signaling the impending demand shock from China before it registered in equity markets.

As a gradual shock unfolds, informed agents trade on localized, field-level information before it is fully reflected in public aggregates (e.g., impact of USDA announcements (Adjemian 2012; A. N. Cao and Robe 2022).The directly exposed contract (e.g., corn) therefore becomes informationally central, serving as a continuously updated signal of the underlying asset (Vives 2008). Market participants in economically or geographically proximate contracts (e.g., wheat) rationally extract this information from price movements to update their own expectations. This cross-asset learning increases contemporaneous conditional dependence among related commodities, while leaving geographically distant or economically unrelated contracts largely unaffected.

A possible narrative is that commercial hedgers - including processors and livestock producers - adjust cross-commodity hedge ratios as relative prices and exposure profiles

[2]While we characterize these markets as "closed" to emphasize their rigid biological constraints, the boundary between physical and financial commodity markets is highly porous in practice. Large commercial merchants actively cross-trade and provide short-term liquidity to financial speculators (W. Kang, Rouwenhorst, and Tang 2020). Furthermore, prior to 2013, major financial institutions maintained massive physical commodity operations that frequently blurred the lines between financial and fundamental price pressures (Bianchi, Fan, and Todorova 2020). Finally, physical arbitrage is not frictionless, as evidenced by historical periods where U.S. agricultural spot and futures prices famously failed to converge at maturity (Garcia, S. H. Irwin, and Smith 2015). It is precisely because of these complex endogenous microstructural linkages that exploiting a strictly exogenous weather shock is necessary for clean identification.

evolve. Because physical risk management is subject to contractual rigidities, production constraints, and uncertainty about final harvest outcomes, hedge reoptimization occurs gradually rather than instantaneously. This implies incremental adjustments in cross-market futures positions, reinforcing contemporaneous linkages over the shock window.

Supply disruptions in a central commodity alter relative prices and activate substitution channels across related markets. Physical substitution (e.g., feed input adjustments) is constrained by logistics, storage, and contractual frictions, while financial substitution operates through spread trading, cross-hedging, and portfolio rebalancing. Because these adjustments intensify as relative prices move further from historical benchmarks, substitution effects can amplify clustering precisely during severe stress episodes. Futures markets incorporate anticipated production adjustments - such as acreage reallocations in subsequent planting seasons (S. Lee 2025) - into current prices, strengthening contemporaneous dependence among economically linked contracts.

These mechanisms build on established frameworks in asset pricing and network theory. Information aggregation follows (Vives 2008; Goldstein and Yang 2022; Ekeland, Lautier, and Villeneuve 2019), where prices of directly exposed assets become informative signals about underlying fundamentals that other markets rationally extract. Sequential hedging adjustments reflect strict limits to arbitrage and slow-moving liquidity (Mitchell, Lasse H. Pedersen, and Pulvino 2007; Duffie 2010), implying that cross-commodity hedge ratios adjust gradually rather than instantaneously. Substitution amplification connects to network models in which shocks to central nodes propagate through structural feedback loops (Elliott, Golub, and Jackson 2014; Acemoglu, Ozdaglar, and Tahbaz-Salehi 2015).

All three channels depend on extended uncertainty resolution. When shocks unfold gradually, cross-asset learning, hedge reoptimization, and substitution dynamics have time to operate, reinforcing contemporaneous conditional dependence. By contrast, fast-breaking financial shocks compress adjustment into short horizons: margin constraints and funding pressures limit arbitrage capital (I.-H. Cheng and Xiong 2014; V. Acharya, Engle, and Richardson 2012), leading to position unwinds rather than coordinated reoptimization. As a result, fast shocks are more likely to generate fragmentation than persistent clustering.

This framework yields three testable predictions regarding network reorganization during slow shocks. First, the centrality of directly exposed commodities - measured via total communicability to capture both direct and indirect propagation paths - should persistently increase as they anchor the market's price discovery process. Second, we

predict structural clustering between the shocked assets and their structurally proximate substitutes. While standard portfolio theory suggests that an asset-specific supply shock should weaken dependence once it is realized, our framework posits that physical substitution and cross-market spread trading forcefully tighten contemporaneous dependence, even for substitutes with minimal direct shock exposure. Third, we expect decoupling of peripheral assets. Commodities lacking fundamental linkages to the shock's epicenter (e.g., coffee) should fragment from the core, as the shocked sector's idiosyncratic volatility overwhelms grain common factor exposures.

Collectively, this topological footprint helps distinguish our slow-shock mechanism from alternative channels. In particular, asymmetric clustering around central commodities is not the pattern one would expect from purely mechanical volatility spillovers. Taken together, these predictions provide a set of empirical implications for assessing the framework.

4. Methodology

4.1 Futures Data

We use daily closing prices and volumes of 10 agricultural futures contracts, from January 1, 2004 to May 3, 2024, obtained from LSEG (Tables 1, 2 in Appendix 1). The selection of these contracts was based on the homogeneity along the time series, that is, the contracts did not experience specification changes for the period as well as there is no presence of structural breaks in the data.[1] The price evolution of commodities is displayed in Appendix 1 with an additional in-depth time-line analysis of the corn market, where biofuel program, market level crises and weather resulted in corn price spikes. There were price increases for all commodities in 2008, great volatility levels throughout the 2010s and surge in cocoa prices in the end of the period - beginning of 2024. In fact, the dramatic increase in cocoa prices in the beginning of 2024 is caused by cocoa shortage due to severe drought in West African regions where 4/5 of the total cocoa crops comes from (Morgan 2024). Average trading volumes are the largest for corn, soybeans, sugar and wheat.

We transform prices in returns r_i, which is expressed as the logarithm price differential,

$$r_i(t) = \frac{\ln F_i(t) - \ln F_i(t - \Delta t)}{\Delta t},$$

[1]These results are available on request.

where $F_i(t)$ is the price of the futures contract at t, and Δt is the time step between the two consecutive trading days which allows to efficiently take into account public holidays and non-trading days on a particular exchange. This results in 4890 return observation points per commodity.

Table 4.1 gives the correlations between all the commodities. Grains are highly connected: there is a soybean complex and corn seems to connect all grains and byproducts. Cocoa US and cocoa UK are also highly correlated with each other. All other correlations are relatively low. In this context, partial correlations and their LASSO penalization should prove relevant.

	Corn	Wheat	Soybeans	SM	BO	Sugar	Cotton	Coffee	Cocoa US	Cocoa UK
Corn		0.58	0.52	0.44	0.41	0.20	0.20	0.17	0.08	0.04
Wheat			0.36	0.30	0.33	0.18	0.20	0.18	0.09	0.06
Soybeans				0.79	0.62	0.18	0.23	0.15	0.10	0.06
Soybean Meal					0.32	0.13	0.17	0.11	0.06	0.03
Soybean Oil						0.19	0.25	0.19	0.13	0.08
Sugar							0.17	0.24	0.14	0.09
Cotton								0.15	0.11	0.07
Coffee									0.16	0.10
Cocoa US										0.77
Cocoa UK										

Table 4.1. Pairwise correlation matrix of commodity futures returns.

4.2 Sparse VAR

First, a stationary zero-mean n-dimensional multivariate time series generated by a pth-order VAR is considered:

$$\mathbf{y}_t = \sum_{k=1}^{p} \mathbf{A}_k \mathbf{y}_{t-k} + \boldsymbol{\epsilon}_t, \quad \boldsymbol{\epsilon}_t \sim \text{i.i.d. } \mathcal{N}(0, \mathbf{C}^{-1}), \tag{4.1}$$

where $\mathbf{A}_k$ and $\mathbf{C}$, the concentration matrix (inverse of covariance matrix) are $n \times n$ matrices.

We adopt the sparse VAR methodology - network estimation for time series (`nets`) - proposed by Barigozzi and Brownlees (2019). It allows for sparsity of autoregressive matrices and of the concentration matrix (inverse of covariance matrix) of the system innovations, which translate naturally into graphs.

On the one hand, we can interpret contemporaneous dependence as an undirected graph. This contemporaneous dependence is measured with partial correlation that is considered between two series. Thanks to the single estimation, the obtained concentration matrix is conditional on the past realizations of the panel and contemporaneous realizations of the

remaining series. This concentration matrix thus represents contemporaneous dependence, purged from their influences and can be transformed into partial correlations as follows:

$$\rho^{ij} = -\frac{c_{ij}}{\sqrt{c_{ii}c_{jj}}}. \tag{4.2}$$

On the other hand, the multivariate predictive Granger structure of the model is present in the sparsity structure of the autoregressive matrices $\mathbf{A}_k$. That is, if $a_{kij} = 0$, for all k, then y_{jt} does not Granger-predict y_{it}[2]:

$$\mathbb{E}[(y_{it+k} - \mathbb{E}(y_{it+k}|\{y_{1t}, \ldots, y_{nt}\}))^2] = \mathbb{E}[(y_{it+k} - \mathbb{E}(y_{it+k}|\{y_{1t}, \ldots, y_{nt}\} \setminus y_{jt}))^2]. \tag{4.3}$$

To graphically represent the interdependence structure, we use network that is defined as a graph $\mathcal{N} = (\mathcal{V}, \mathcal{E})$, where $\mathcal{V}$ is the set of vertices, representing the components of $\mathbf{y}_t$, and $\mathcal{E}$ is the set of edges.

The contemporaneous network is constructed as an undirected network $\mathcal{N}_C = (\mathcal{V}, \mathcal{E}_C)$, where an undirected edge between i and j represents a non-zero partial correlation between the two variables:

$$\mathcal{E}_C = \{(i, j) \in \mathcal{V} \times \mathcal{V} : \rho^{ij} \neq 0\}.$$

The Granger network is constructed as a directed network $\mathcal{N}_G = (\mathcal{V}, \mathcal{E}_G)$, where an edge from node i to node j indicates that i Granger-predicts j:

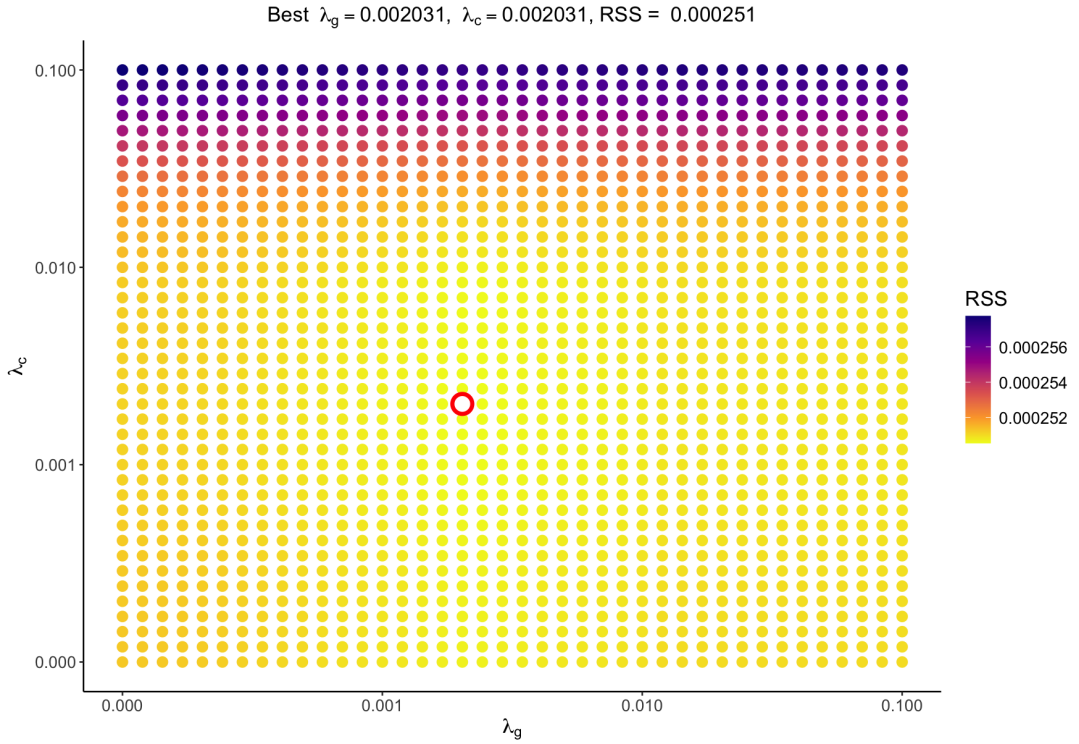
$$\mathcal{E}_G = \{(i, j) \in \mathcal{V} \times \mathcal{V} : a_{kij} \neq 0, \text{ for at least one } k \in \{1, \ldots, p\}\}.$$

`nets` relies on a single estimation of those two components with LASSO penalization, allowing for different penalizing intensities for each, λ_g for the autoregressive matrices and λ_c for the concentration matrix respectively.[3] To select the appropriate shrinkage parameters, we conduct a two-dimensional grid search over a range of candidate values.

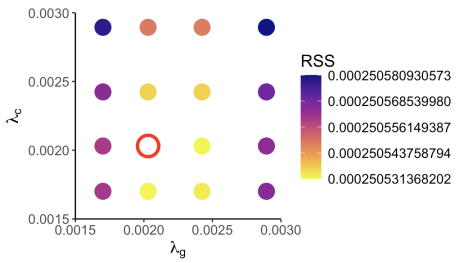
[2]In line with the original NETS formulation (Barigozzi and Brownlees 2019), directed edges are labeled as instances of Granger causality, since they correspond to non-zero autoregressive coefficients in the sparse VAR. In practice, these links represent reduced-form predictive directionality: past values of one series forecast another, conditional on the entire high-dimensional system. Because estimation relies on sparsity and shrinkage, and edges are defined mechanically from coefficients rather than explicit variance-reduction tests, not all links need correspond to full Granger-causal relations. We therefore prefer the term directionality to stress predictive influence rather than strict causal identification. Directed edges reflect non-zero VAR coefficients ($a_{kij} \neq 0$) indicating Granger predictability, while contemporaneous links come from partial correlations of VAR innovations; both are reduced-form.

[3]Refer to Barigozzi and Brownlees (2019) for the details on the model, estimation, algorithm and theory behind this methodology.

For each parameter combination, the model is trained on the first 75% of the sample and its predictive performance is evaluated on the remaining 25% using the out-of-sample residual sum of squares (RSS). The optimal pair of regularization parameters is selected as the one that minimizes the prediction error. Using these optimal values, the final model is re-estimated on the entire dataset. Figure 4.1 shows the heatmap of residual sum of squares (RSS) values obtained from this grid search. The grid was constructed on a logarithmic scale for 40 values for each λ multiplying to 1600 λ pairs. The range of the values from 0.0001 to 0.1 was chosen based on a previous estimation where coarser grids (e.g., $\lambda = 1$ or 2) yield higher RSS.



(a) RSS minimisation over the full λ_g–λ_c grid. The red circle indicates the optimal pair.



λ_g	λ_c	RSS
0.002030918	0.002030918	0.0002505314
0.002424462	0.002030918	0.0002505319
0.002030918	0.0017012543	0.0002505319
0.002424462	0.0017012543	0.0002505330
0.002030918	0.0024244620	0.0002505363

(b) Zoom around the optimum.

Figure 4.1. Residual sum of squares (RSS) minimisation with respect to the shrinkage parameters λ_g and λ_c.

As seen in Figure 4.1b, our results reveal one optimum.[4] The minimum out-of-sample RSS is 0.0002505314, achieved for $\lambda_g = \lambda_c = 0.002030918$. That said, the differences in predictive performance across the top-ranked parameter pairs are negligible, and the resulting networks are highly stable. Both the number and intensity of estimated links remain virtually unchanged, underscoring the robustness of the NETS procedure to minor variations in regularization.

4.3 Difference-in-Differences (DiD)

Drought as an exogenous slow shock As discussed in Section 3, the duration of shocks may not be apparent if their impact is not immediate. We have such an example with droughts, which are not point events. The by far strongest drought in the U.S. affecting our system over the twenty-year period was the 2012 drought.[5] The gradual information revelation window during the drought creates opportunities to observe dynamic reorganization.[6] We thus implement a DiD design centered on the 2012 U.S. drought (treatment period) as a natural experiment. It is indeed plausibly exogenous supply shock: meteorological conditions are orthogonal to market structure or trading behavior. We conduct the same analyses for other years, which include some droughts, for comparison purposes.

Network specifics Classical DiD analysis presents some caveats: treatment effects may spill over through network links (Jetsupphasuk, D. Li, and Hudgens 2025), which are particularly prominent in our markets. Indeed, the shock struck the system's most central commodities. Corn and soybeans represent the largest components of U.S. cropland and function as bridge assets linking grains, biofuels, livestock feed, and international markets. A disturbance to these core nodes generates heterogeneous exposure across the network. Consequently, we apply the doubly robust DiD estimator of Callaway and Sant'Anna (2021), which has become the benchmark approach for panel data settings with

[4]We have similar outcome with cross-validation results for rolling window NETS estimations. These results are available upon request.

[5]The U.S. Drought Monitor classified 65% of the contiguous United States under drought conditions by July 2012, with exceptional drought (D4 classification) concentrated in Illinois, Iowa, Nebraska, Indiana, and Minnesota - states accounting for 60% of U.S. corn production and 50% of soybean production but only 15% of wheat production (USDA NASS).

[6]USDA's June 10, 2012 crop condition report showed only 54% of corn rated good and 12% excellent (USDA, NASS 2012a). By July 22, just 23% remained good and 3% excellent (USDA, NASS 2012b) - the worst reading since 1986 - confirming severe and widespread damage. USDA yield expectations deteriorated sharply over the summer and were revised down to 123.4 bushels per acre for corn by early August; final yields were confirmed after harvest at 123.4 bushels per acre for corn and 39.6 bushels per acre for soybeans in the January 2013 Crop Production summary.

heterogeneous treatment effects and staggered timing. The estimator avoids the negative-weight and aggregation biases associated with traditional two-way fixed effects and delivers group-time average treatment effects under transparent parallel trends assumptions.

This framework needs some detailing: we need to define the variable investigated (connectivity), the treatment window and the anchor. In order to assess the effect of drought over time, we conduct rolling-window estimations of `nets`, thus getting time series of predictive matrices and partial correlation matrices. Since we have two types of networks (predictive and contemporaneous), we apply DiD to both and focus on the contemporaneous one for the explanations below.

Baseline identification Our baseline treatment window for drought is 1 Jun-31 Aug. This methodology requires defining an anchor in the system, to which other node connectivity (our variable of interest) will be assessed. We select climate-relevant anchor contracts $\mathcal{A} \subset \{1, \ldots, K\}$, affected by the drought, corn–wheat and soybeans–oil–meal. Identification relies on a pre-treatment parallel trends assumption. From the partial correlation matrix $\widehat{\mathbf{P}}_t = (\hat{\rho}_{ij,t})$, we define

$$Y_{jt} = \max_{a \in \mathcal{A}} |\hat{\rho}_{ja,t}|, \tag{4.4}$$

which captures the strongest single anchor linkage. In addition, we remove contract-specific linear pre-trends separately for each candidate year y using only information from the corresponding pre-shock period $\mathcal{T}_y^{\text{pre}}$ (Autor, Kerr, and Kugler 2007; Dube, Lester, and Reich 2010; Liu and Sun 2019). Let $\tau_{t,y}$ denote a time index normalized to zero at the beginning of $\mathcal{T}_y^{\text{pre}}$. For each contract j, we estimate

$$Y_{jt} = \alpha_{j,y} + \beta_{j,y}\tau_{t,y} + \varepsilon_{jt}, \qquad t \in \mathcal{T}_y^{\text{pre}}, \tag{4.5}$$

and define the detrended outcome

$$\tilde{Y}_{jt} = Y_{jt} - \hat{\beta}_{j,y}\tau_{t,y}. \tag{4.6}$$

This procedure preserves cross-sectional level differences while removing contract-specific linear drifts in connectivity that could violate parallel trends (S. J. Lee and Wooldridge 2023; Arkhangelsky et al. 2021).

Treated vs. control groups For each year y in the sample (2006–2023), we define the treated (control) group as the non-anchor markets with High (Low) connectivity. Let $\mathcal{T}_y^{\text{pre}}$ denote the one-year period preceding the start of the corresponding climate window. For each non-anchor contract j, we compute average pre-shock exposure

$$\bar{Y}_{j,y}^{\text{pre}} = \frac{1}{|\mathcal{T}_y^{\text{pre}}|} \sum_{t \in \mathcal{T}_y^{\text{pre}}} \tilde{Y}_{jt}.$$

Let $Q_q(\bar{Y}_y^{\text{pre}})$ denote the q-th quantile of $\{\bar{Y}_{j,y}^{\text{pre}}\}_j$. We then classify contract j as High (treated) if $\bar{Y}_{j,y}^{\text{pre}} \geq Q_q(\bar{Y}_y^{\text{pre}})$. Our identifying assumption is therefore that detrended exposure $\tilde{Y}_{jt}(0)$ would have evolved in parallel across groups absent the shock.

Robustness We take several variations and end up with 21 scenarios tested. For each scenario s, exposure, group assignment, and detrended outcomes are constructed using only pre-shock information. We then re-estimate both the average post-shock effect and the dynamic event-time profile using the CSA estimator (Callaway and Sant'Anna 2021). Robustness is assessed based on the qualitative stability of sign, magnitude, and statistical significance across the pre-specified scenario grid in Table 5.2.

5. Empirical Results

We begin by investigating the organization of the network over the whole period by estimating static NETS for contemporaneous and predictive Granger networks. We proceed with dynamic analysis of time variation in network topology using centrality and network connectivity intensity measures, where fast shocks can be observed. Finally, we display the results of the novel difference-in-differences design across years and specifications to assess how slow building shock - 2012 U.S. drought - affects contemporaneous dependence.

5.1 Static connectedness

The estimated contemporaneous network, constructed from the inverse covariance structure of commodity returns, reveals organization containing three distinct clusters for the whole period (Figure 5.1), with the Fruchterman and Reingold (1991) layout algorithm indicating the real position of commodities in space.[1] We observe the presence of mostly positive

[1]The Fruchterman–Reingold algorithm is a force-directed layout method that positions nodes by simulating attractive forces along edges and repulsive forces between all nodes. Nodes that are more strongly or densely connected tend to be placed closer together, revealing clusters and natural sectorization in the network.

contemporaneous price co-movements even after accounting for dynamic (lagged) effects in the optimization problem. The commodities with multiple strong connections are corn, soybeans and soybean oil, where all soy goods are closely linked together, and cotton is closely related to soybean oil which is also indicative from the correlation matrix (Table 4.1). The connection of cotton and soybean oil is possibly due to production of cottonseed meal - a by-product of oil from cotton seeds - is known to be a partial substitute for soybean meal (J. Wang et al. 2020). Cocoas from both markets - US and UK - are closely connected and positionned apart, and cocoa UK is isolated on the periphery of the graph as being the only non-U.S. commodity. Wheat is tightly linked to corn forming another smaller cluster. Corn-sugar connection is likely due to high fructose corn syrup that is a substitute for sugar (OECD and Food and Agriculture Organization of the United Nations 2018, p. 143).

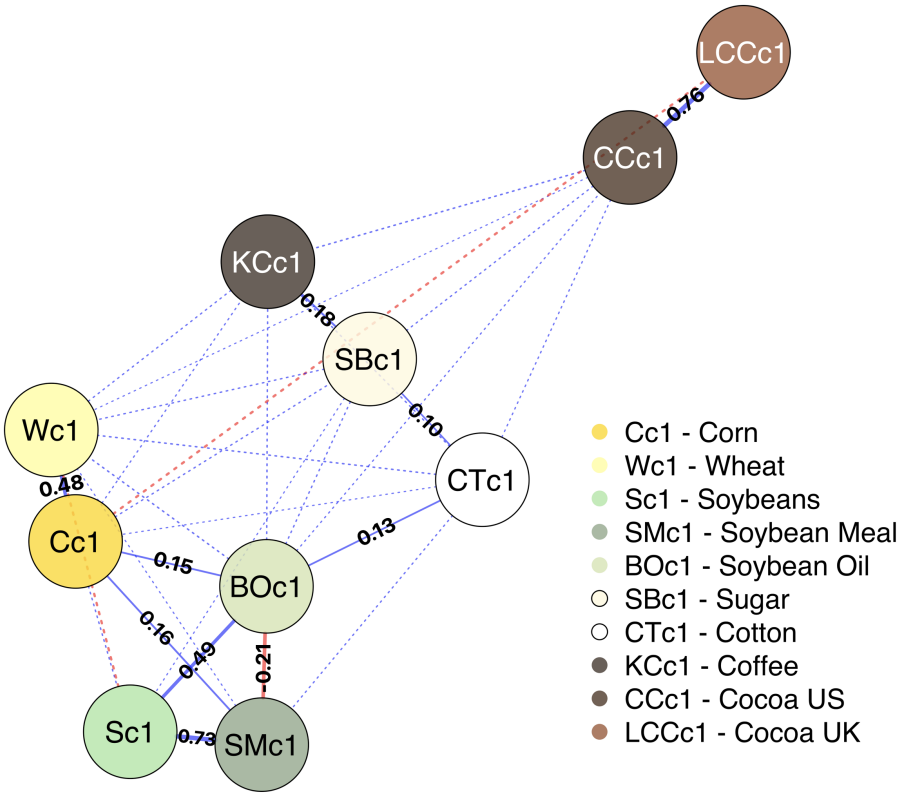


Figure 5.1. Comtemporaneous graph

NETS for the whole period with $\lambda_g = 0.0020309$ and $\lambda_c = 0.0020309$ where numerical values stand for partial correlations (ρ), and thicker lines represent stronger partial correlations than thinner and dotted links, and red links stand for negative partial correlations. The nodes are arranged using a Fruchterman-Reingold layout.

This topology possibly indicates that soybeans and soybean oil are strongly connected to the remaining network. Interestingly, the partial correlation between soybean meal and soybean oil is negative knowing that both soy derivatives have a very weak pairwise

correlation among each other. This is likely due to optimization coming from crushing process[2]. In general, connections among grains are stronger than among softs, but softs like sugar, cotton and coffee have equally strong links with all remaining commodities suggesting for a dense network overall.

Table 5.1 displays the estimated autoregressive matrix - predictive directionality network - which captures the structure of lagged predictive relationships among commodity returns. These relationships are derived from the first-lag autoregressive coefficient matrix $\hat{A}_1$ of a sparse vector autoregressive (VAR(1)) model. In this setting, a directed edge from commodity j to commodity i indicates that past returns of commodity j help predict current returns of commodity i which corresponds to a non-zero entry in position (i, j) of the estimateed $\hat{A}_1$ matrix. Each row represents the dependent variable, and each column corresponds to a predictor (lagged commodity). For example, the entry in row `SBc1` (Sugar) and column `Sc1` (Soybeans) shows how lagged returns of soybeans positively predict current returns of sugar.

A few key patterns can be observed. Soybeans (Table 5.1) appear as major transmitter of lagged effects, with notable connection with soybean oil and soybean meal. Similarly, soybean oil negatively predicts soybean meal and vice versa. Corn also transmits to wheat, while soft commodities, especially coffee, generally receive more signals than they transmit. Cotton and sugar receive from soybeans. Overall, grains emerge as primary transmitters of lagged price reduced-form shocks, while softs act predominantly as receivers, with the exception of wheat and soybean meal, grains that are not used for energy production.

The relative sparsity of the predictive network compared to the dense contemporaneous

[2]The process by which soybeans are transformed into by-products - soybean meal and soybean oil - is known as crushing, and the profitability of this process is captured by the crush spread, which is actively traded by financial participants. While weather shocks affect the availability of raw soybeans, the prices of soybean meal and oil are primarily driven by crushing economics: processors only increase crushing if the crush spread is sufficiently profitable, meaning the combined value of oil and meal outweighs the cost of soybeans. Additionally, soybean oil prices are closely tied to biofuel policies, vegetable oil markets and oil prices while soybean meal prices depend heavily on livestock supply, as meal is a key input for animal feed. Inventory levels of both oil and meal also buffer short-term supply shocks; while stocks are not directly analyzed in this paper, they could represent a meaningful avenue for future research to better understand co-product pricing dynamics.

For example, according to the USDA (U.S. Department of Agriculture, Foreign Agricultural Service 2025), in the 2024/25 fiscal year, the U.S. is projected to account for approximately 28% of global soybeans production, totaling 118.84 million metric tons. The July 2025 WASDE report U.S. Department of Agriculture, Office of the Chief Economist (July 2025) forecasts U.S. soybeans production at 4.3 billion bushels, with a crush volume of 2.54 billion bushels. Of the resulting soybean oil, an estimated 15.5 billion pounds is expected to be allocated for biofuels production. Given that one bushel of soybeans yields approximately 11 pounds of soybean oil and 44 pounds of soybean meal (CME Group 2025), this implies that approximately 33% of the total soybeans production in 2025 will be directed toward biofuels, calculated as $15.5 \div 11 \div 4.3 \approx 0.33$.

Receiver ↓	**Transmitter →**									
	Cc1	Wc1	Sc1	BOc1	SMc1	SBc1	CTc1	KCc1	CCc1	LCCc1
Corn	–	–	–	–	–	–	–	–	–	–
Wheat	-0.00486	–	–	–	–	–	–	–	-0.01572	–
Soybeans	–	–	-0.06336	–	–	–	–	–	–	–
Soybean Oil	–	–	–	–	-0.03566	–	–	–	–	–
Soybean Meal	–	–	0.03169	-0.01158	-0.04154	–	–	–	–	–
Sugar	–	–	0.03055	–	–	–	–	–	-0.00270	–
Cotton	–	–	-0.01165	–	–	–	0.05769	–	–	0.00337
Coffee	–	0.02999	0.04052	–	-0.04182	–	–	-0.02648	–	–
Cocoa US	–	–	-0.03661	–	0.01193	–	–	–	–	–
Cocoa UK	–	–	–	–	–	–	–	–	–	–

Table 5.1. Estimated $\hat{A}_1$ matrix of Granger predictive coefficients. Columns correspond to transmitting variables and rows to receiving variables. Entry (i, j) measures the effect of variable j on variable i. Entries below 0.001 are shown as "–".

structure is consistent with the high degree of informational efficiency in financialized commodity markets. As liquid futures markets serve as rapid aggregators of dispersed global information (I.-H. Cheng and Xiong 2014), prices tend to incorporate new signals almost instantaneously, often resulting in immediate repricing rather than lagged predictability (Fama and French 1987; Taşkin, Cagli, and Evrim Mandaci 2021). Consequently, the transmission of information largely occurs within the trading day, rendering daily autoregressive coefficients statistically insignificant for many pairs.

5.2 Dynamic Connectedness

5.2.1 Centrality

Centrality measures allow to detect the central asset in the system that plays a role of shock transmission mechanism in global networks. In our case, central agricultural commodities would have implications on clustering of the network, and on the nature of price formation processes coming from external shocks, as for example, grains are more likely to absorb and pass on energy shocks.

While simple degree centrality provides an intuitive measure of local connectivity by counting direct linkages, it is theoretically insufficient for capturing systemic risk in financialized commodity markets. A commodity with high degree centrality may simply exist within a closed local cluster, whereas a systemically critical asset acts as a bridge, transmitting volatility through long chains of indirect dependencies. To capture this global propagation potential, we employ total communicability measure of centrality (Benzi and Klymko 2013).

Unlike degree centrality, total communicability aggregates infinite-length walks across

the network, penalizing longer paths to reflect information decay. We compute it for both the contemporaneous ($\mathcal{N}_C$) and predictive ($\mathcal{N}_G$) matrices. This allows us to identify not merely which commodities have the most direct neighbors, but which possess the structural capacity to transmit external shocks deep into the agricultural complex through indirect feedback loops that simple local measures ignore.

Let A be the adjacency matrix of the network. The k^{th} power A^k enumerates the number of walks of length k between every pair of vertices. To capture systemic reverberation while preventing the measure from diverging due to infinite feedback loops, we weight each term by $\beta^k/k!$. This factorial penalty serves a dual purpose: mathematically, it ensures the power series converges to the matrix exponential $\exp(\beta A)$; economically, it captures the natural decay of risk transmission. While shocks can propagate globally, their intensity diminishes exponentially as they pass through intermediate nodes, ensuring that direct exposures remain the primary drivers of centrality (Benzi and Klymko 2013):

$$C_i = \sum_{j=1}^{N} [\exp(\beta A)]_{ij} = \sum_{j=1}^{N} \sum_{k=0}^{\infty} \frac{\beta^k}{k!} [A^k]_{ij},$$

where $\beta > 0$ is a scaling parameter controlling the relative importance of long versus short transmission paths.

In what follows, we adapt the total communicability to NETS model. To do this, we propose two modified communicability measures. First, for the contemporaneous network structure, we compute communicability based on the absolute value of the partial correlation matrix $|\boldsymbol{\rho}|$[3], removing self-loops before and after the exponential:

$$\text{TC}^{(\rho)} = \exp\left(\beta(|\boldsymbol{\rho}| - I)\right) - I = \sum_{k=1}^{\infty} \frac{\beta^k}{k!} (|\boldsymbol{\rho}| - I)^k.$$

Second, for the predictive Granger network implied by the VAR(1) model, we define communicability using the absolute value of the estimated autoregressive matrix $A^{(1)}$, again excluding self-interactions:

$$\text{TC}^{(A)} = \exp\left(\beta[|A^{(1)}| - diag(|A^{(1)}|)]\right) - I = \sum_{k=1}^{\infty} \frac{\beta^k}{k!} \left(|A^{(1)}| - diag(|A^{(1)}|)\right)^k.$$

[3]We prioritize absolute values over signed coefficients to capture the total magnitude of systemic connectivity. Since partial correlations and autoregressive coefficients can be negative, summing signed values would cause offsetting effects that obscure the true intensity of network linkages. Results using signed coefficients are provided in the Appendix 3.

In both cases, the diagonal is subtracted before taking the exponential to eliminate structural self-loops. This adjustment is necessary because standard network theory assumes simple graphs with zero diagonals. However, estimated financial matrices inherently contain non-zero diagonal elements representing idiosyncratic persistence (autoregressive coefficients) or self-correlation. While retaining these self-loops could theoretically be justified - as high internal persistence amplifies the duration of a shock within a node - we remove them to disentangle systemic centrality (transmission to others) from idiosyncratic memory. This ensures that a commodity is ranked as central based on its connectivity to the system rather than its own volatility persistence. The matrix I is subtracted afterward to ensure that the minimum possible centrality is zero rather than one, by removing the contribution of trivial zero-length walks included in the exponential's zeroth-order term. The resulting total communicability centralities can then be computed as row- or column-sums of the respective matrix for out- and in-centrality:

$$\text{Out}^{\hat{A}_1}(j) = \sum_i \hat{A}_{1,ij}, \qquad \text{In}^{\hat{A}_1}(j) = \sum_i \hat{A}_{1,ji}.$$

We set the scaling parameter $\beta = 1$, consistent with the standard formulation of total communicability in weighted networks (Benzi and Klymko 2013; Estrada and Hatano 2008).[4] Unlike binary adjacency matrices where links represent mere existence, our matrix elements consist of estimated partial correlations and autoregressive coefficients that inherently quantify the strength of transmission. Since these edge weights already capture the intensity of information flow, the resulting power series naturally downweights weaker transmission paths without requiring further exogenous decay via the scaling parameter.[5]

In Figure 5.2,[6] soybeans experience the highest level of centrality. Soybean oil, soybean meal, corn and wheat also demonstrate pronounced fluctuations in communicability. In contrast, commodities such as cotton, sugar and coffee display periods of limited communicability, suggesting phases of relative independence from the broader market network. Cocoa US and UK have larger centrality due strong mutual interconnections. This underscores that grains are more connected with the network than softs and that there are periods of heightened systemic connectivity versus periods dominated by idiosyncratic factors. Overall, the periods of centrality intensity are cyclical with persistent ordering.

[4]While lower values of β can be employed to impose additional attenuation on longer walks, such adjustment is unnecessary in our context.

[5]Although we use a range of β parameters in the Difference-in-Differences analysis (Section 5.3.1).

[6]Same conclusion for signed values. See the results in Appendix 3.

In practice, these centrality magnitudes serve as a proxy for the network's amplification factor. Because total communicability sums infinite walks weighted by the matrix exponential, the difference between a score of 1-2.5 for soybeans and between 0 and 0.5 for sugar is non-linear and structurally significant. A value of 2 implies that a shock to soybeans does not merely dissipate - it reverberates through multiple feedback loops and indirect pathways, effectively acting as a "super-spreader" event (Benzi and Klymko 2013). In contrast, a score between 0 and 0.5 (as for sugar, cotton, coffee) indicates topological isolation, where volatility decays rapidly before reaching the broader system. Therefore, corn (between 0.5 and 1.5) occupies, in a tandem with wheat, a critical intermediate tier: it is sufficiently integrated to transmit shocks within the grain complex, but lacks the hyper-centrality of soybeans required to trigger the system-wide cascades described by (Acemoglu, Ozdaglar, and Tahbaz-Salehi 2015).

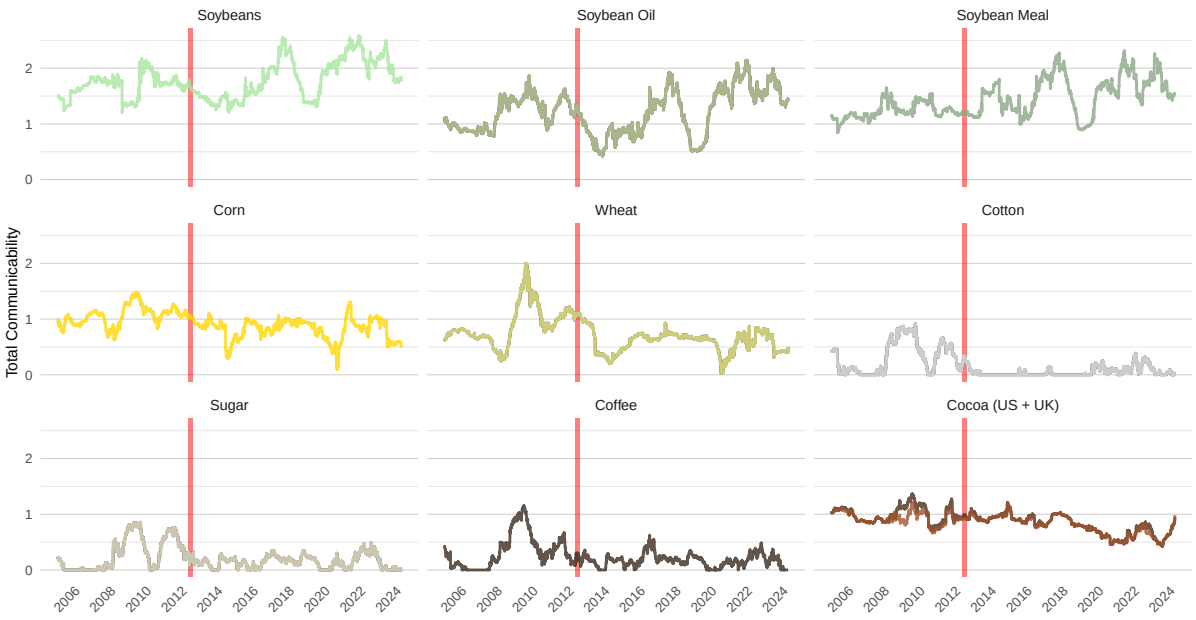


Figure 5.2. Contemporaneous graph
Total communicability of the contemporaneous graph - magnitude ($|\rho|$). Red vertical line marks 2012 U.S. drought

Our analysis requires disentangling genuine systemic dominance from topological artifacts. We acknowledge that a portion of the high centrality observed in specific commodities is mechanically driven by local clustering. Total communicability sums infinite walks so tightly coupled arbitrage pairs create feedback loops that inflate centrality scores for all members of the cluster. This is empirically evident in the softs sector: cocoa US and cocoa UK exhibit elevated and nearly identical centrality scores, reflecting a closed arbitrage loop, while isolated softs (coffee, sugar, cotton) remain peripheral with

low communicability. Similarly, the strong bidirectional linkage between corn and wheat contributes to their shared high centrality.

However, the internal topology of the soybean complex reveals that high communicability scores do not always equate to independent systemic weight. We observe that soybeans and soybean meal share a hyper-central profile, whereas soybean oil appears less central. Possibly, the dominance of meal is artificially inflated by its extreme partial correlation with raw soybeans ($\rho = 0.73$), the highest in the sample after cocoa cluster. Because meal acts as a very close reflection of the soybeans price, it mechanically duplicates the centrality of the parent node without adding distinct connectivity to the wider network. In contrast, soybean oil, despite its lower raw centrality score, exhibits a distinct topological role. It is negatively correlated with soybean meal ($\rho = -0.21$) but serves as the critical bridge to the energy sector (S. H. Kang, Tiwari, et al. 2019). Consequently, we identify soybeans, corn, and soybean oil as the inherently central nodes of the agricultural network. These three commodities act as the structural backbone that might link the agricultural system to global energy markets via the biofuel channel (Paris 2018), whereas soybean meal primarily reinforces internal cluster density rather than propagating systemic shocks.

The directed Granger total communicability is shown in figures 5.3 and 5.4.[7] Soybeans transmit the largest portion of shocks, followed by soybean oil and soybean meal in the beginning of the period. Corn and wheat also transmit shocks but at a lower scale. Softs almost do not play a role of an autoregressive shock transmitter, meaning that these contracts are not influencial enough for systemic spillovers. However, softs receive substantial amount of information (Figure 5.4). Interestingly, soybeans played a role of a recipient of shocks one time in 2009 which coincides with the drop in their contemporaneous communicability. That is, soybeans and its derivatives are clearly the most central assets, and although corn transmits shocks, it surprisingly also receives a lot of information with a peak in 2014. Cotton, coffee, and sugar are constant "receivers", cocoa US and UK neither receive nor transmit a lot.

This analysis shows that some futures contracts are more crucial for systemic risk than others. In particular, the importance of soybeans stems not only from the fact that it is a heavily traded market for speculation (crushing, arbitrage with Chinese or Brazilian soybeans), but also because soybeans are important for several industries.[8]

[7] Similarly, the predictive autoregressive graph shock transmission and reception with signed values is displayed in Appendix3.

[8] Only a small percentage of soybeans is used for human food such as tofu or soy milk, and soybeans are also used directly for animal feed. 95% on average of produced soybeans is used for soybean meal -

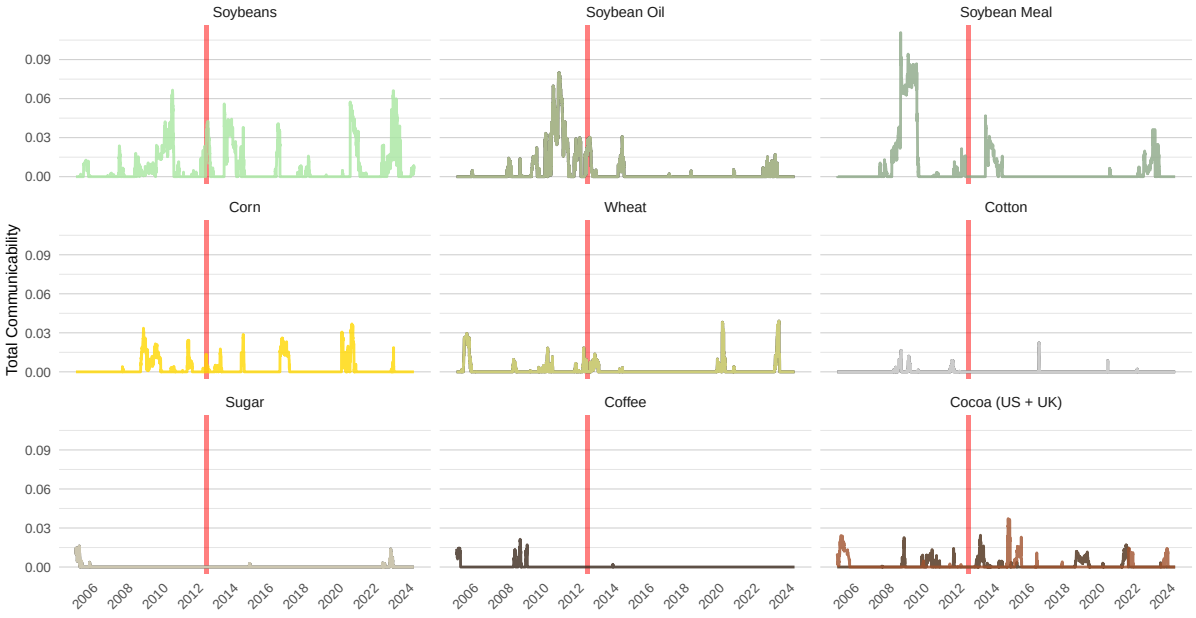


Figure 5.3. Predictive graph transmission
Total communicability of the predictive graph - magnitude of shock transmission ($|A1|$). Red vertical line marks 2012 U.S. drought.

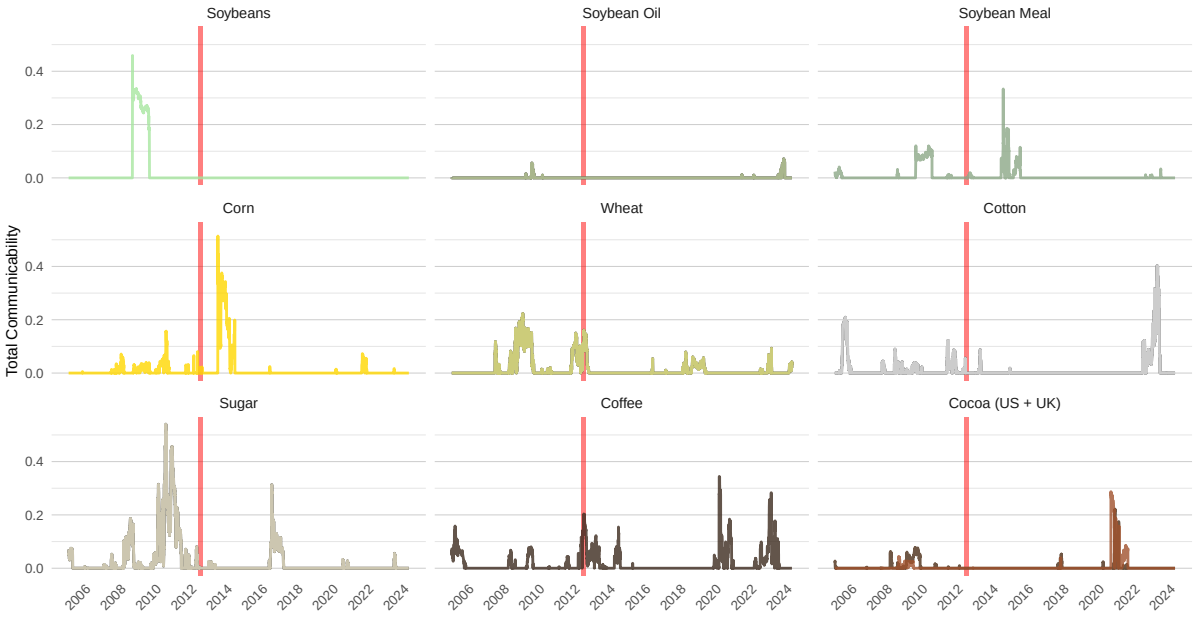


Figure 5.4. Predictive graph reception
Total communicability of the predictive graph - magnitude of shock reception ($|A1|$). Red vertical line marks 2012 U.S. drought.

5.2.2 Network Intensity - shock velocity

To quantify the evolving connectedness of the commodity system, we define Network Intensity as the aggregate magnitude of dependence, calculated as the sum of absolute partial correlations for the contemporaneous network ($\mathcal{N}_C$) and absolute autoregressive coefficients for the predictive network ($\mathcal{N}_G$).

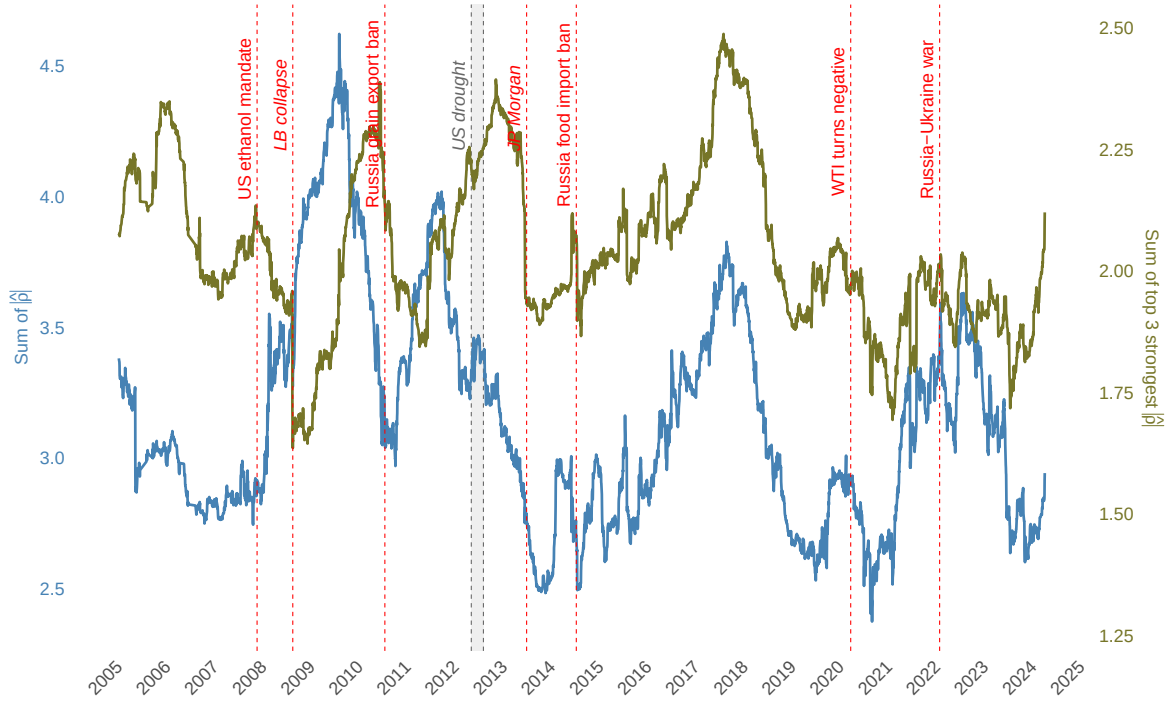


Figure 5.5. Rolling sum of partial correlations

240-Day rolling sum of all links (blue) and of top 3 strongest $|\hat{\rho}|$ (green) with the mean of 360-Day cross-validated lambdas. See a deeper explanation of chosen events in Appendix1.

Figure 5.6 traces the trajectory of contemporaneous integration. The blue line (total network intensity) exhibits a cyclical behavior generally consistent with the waves of financialization documented by I.-H. Cheng and Xiong (2014) and Basak and Pavlova (2016). We observe a secular rise in connectivity peaking during the Global Financial Crisis (2008–2009), followed by elevated integration during the commodity boom (2011–2012) and the post-pandemic inflationary period (2021–2024). This baseline high connectivity reflects the structural integration of agricultural markets.

or other animal feeds, soybean oil or biodiesel. According to United Soybean Board (United Soybean Board 2024), 50% of biodiesel consumption in 2017/2018 exploited 3.24 million metric tons of soybean oil, or the oil from 667.44 million soybean bushels, and an overall of 4412 million bushels of soybeans were produced in 2017 making biodiesel 15% of total US production of soybeans (U.S. Department of Agriculture, Economic Research Service 2024). The production of biodiesel from soybeans increases the overall supply of soybeans. That is, due to the dual-use nature of soybeans, which can be processed into both oil and meal, an increase in the demand for soybean oil for biodiesel results in a greater availability of soybean meal that is subsequently used in animal feed production.

However, a granular analysis of the strongest linkages (green line, sum of top 3 strongest partial correlations) reveals that a few fast-breaking surprise shocks trigger immediate short-lived network fragmentation.[9] We identify distinct statistical "structural breaks" where contemporaneous dependence sharply contracts following (1) financial or (2) geopolitical supply events.[10] Precisely, the collapse of Lehman Brothers (Sept 2008) and the U.S. regulatory pressure followed by JPMorgan's sudden exit from physical commodity trading (July 2013)[11] triggered immediate drops in partial correlations. Similar fragmentation occurred following the Russian grain export ban (August 2010) and the Russian food import ban (August 2014). These announcements arrived as instantaneous supply disruptive signals, and the sharp drop in connectivity likely suggests that during such "fast" shocks, the affected assets (e.g., wheat) idiosyncratically decouple from the system to process the new information, consistent with the efficient price discovery mechanisms (Fama 1965).

This contraction of contemporaneous dependence during surprise events contrasts sharply with the 2012 U.S. Drought (a slow-building shock), where our hypothesis is to observe network clustering, and also the implementation of the U.S. Ethanol Mandate that caused grain price increases over several years (Lark et al. 2022). Over these periods, where information regarding supply constraints was revealed sequentially rather than instantaneously, we do not observe fragmentation; instead, the extended time horizon possibly allows substitution mechanisms and hedging rebalancing to tighten cross-market linkages. This divergence substantiates our theoretical proposition: slow physical shocks provide the necessary latency for agents to propagate stress through the network, whereas fast financial surprises exhaust arbitrage liquidity, causing the network to momentarily fracture.

The onset of the Russia-Ukraine war constitutes a unique outlier: despite being a distinct "Fast" shock, it did not trigger the network fragmentation typical of crises. Instead, the invasion generated a simultaneous fundamental supply shock across the energy-fertilizer-grain nexus, causing prices to move in unison rather than decouple (Figure 1). This maintenance of network integrity confirms that the decoupling observed

[9]The statistical analysis of largest daily variations in contemporaneous and Granger graphs top 3 links intensity level are discussed in Appendix 3. These results show that the strongest changes actually appear around the selected announcement days.

[10]The description of each event in Figure 5.6 is provided in Appendix 1.

[11]On July 26, 2013, JPMorgan announced its exit from physical commodity trading amid regulatory pressure, marking the end of the investment bank era in physical supply chains (Reuters 2013). See more on that in Appendix 1.

during financial crises is driven by liquidity distress, whereas the 2022 event reflected a functioning market efficiently transmitting a systemic physical price shock (Guo et al. 2023).

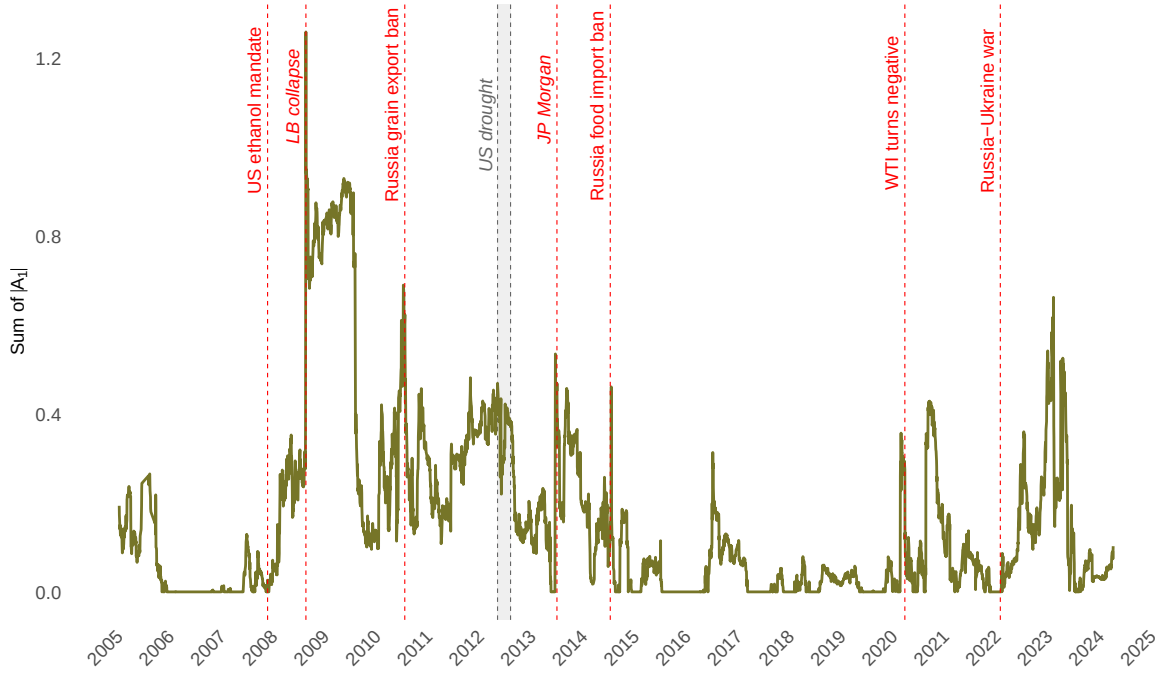


Figure 5.6. Rolling sum of autoregressive coefficients
240-Day rolling sum of $|A1|$ with the mean of 360-Day cross-validated lambdas

Complementing the contemporaneous view, Figure 5.6 illustrates the evolution of Predictive Network Intensity, defined as the aggregate magnitude of the autoregressive coefficient matrix ($|A_1|$). In a frictionless market with infinite arbitrage capital, price adjustments to public news should be instantaneous; therefore, we interpret spikes in predictive intensity as episodes where informational efficiency breaks down, forcing sequential rather than simultaneous repricing.

Crucially, the 2012 U.S. Drought - the most severe physical supply shock of the century - is absent from these predictive spikes. The Granger network intensity remained stable throughout the summer of 2012. This null result supports the hypothesis that markets process "slow-building" physical risks efficiently. Agents continuously update beliefs regarding weather outcomes based on sequential signals (e.g., crop condition reports). Because this information accrues gradually, traders incorporate it into prices contemporaneously. There is no single "surprise" large enough to exhaust liquidity and trigger the lagged cascades observed during financial crises (Letta, Montalbano, and Pierre 2022).

Consequently, aggregate dynamic network measures are insufficient for identifying any systemic impact of slow-onset climate (or geopolitical) risks. Because drought information is incorporated smoothly via the contemporaneous channel ($\mathcal{N}_C$) rather than the lagged channel ($\mathcal{N}_G$), possible systemic reorganization triggered by the 2012 drought is obscured in aggregate indices.

5.3 Slow moving and latent systemic risk

To uncover if physical stress reshapes the market's topology, we move beyond aggregate network length to a granular Difference-in-Differences (DiD) identification of centrality, testing whether drought-exposed commodities (corn, soybeans) become structurally more central relative to the unexposed periphery.

Table 6 in Appendix 3 provides model-free statistical evidence consistent with network clustering under physical stress. We compute the pairwise difference between the correlation matrix during the drought period (May 2012–June 2013) and the full-sample baseline to isolate the shock-specific covariance structure. The grain complex exhibits marked intensification of internal comovement (e.g., corn–wheat correlations increase by 0.11 and soybeans–meal by 0.13), consistent with tighter substitution linkages and shared supply constraints. In contrast, soft commodities (cotton, sugar, coffee) decouple from the grain core, as reflected in systematically negative differentials (e.g., soybeans–cotton declines by 0.14). These patterns constitute preliminary evidence of clustering.

We further validate the severity of the physical shock by estimating the direct return sensitivity of commodities during the drought window (June 1–September 1). Table 7 in Appendix 3 shows that drought-exposed grains experienced statistically significant positive price responses, with corn ($t = 2.16$, $p = 0.03$) and soybeans ($t = 1.92$, $p = 0.05$) exhibiting distinct appreciations. By contrast, soft commodities such as coffee, cocoa, and sugar display no statistically significant sensitivity, confirming that the shock was economically concentrated in the grain complex. The observed tightening in network connectivity therefore coincides with a fundamental repricing driven by physical scarcity.[12]

5.3.1 Difference-in-differences

We present difference-in-differences estimates of the drought's impact on network connectivity for each year from 2006–2023, benchmarking the 2012 event against the full sample of potential weather shocks (Figures 5.7 and 5.8). For each year, we estimate

[12]Applying the same correlation-difference and sensitivity analyses to other candidate years does not reveal comparable clustering patterns. Detailed results are available upon request.

21 pre-specified specifications (Table 5.2). These specifications systematically vary the definition of the event window, the exposure threshold separating High and Low contracts, the length of the pre-event baseline period, the exposure aggregation rule, the detrending procedure, and where applicable - the total communicability parameter β.

Spec.	Drought window	Threshold	Pre (days)	Aggregation	Detrending	Comm. β
1	1 Jun-31 Aug	0.50	365	Max pcorr	Linear	-
2	1 Jun-31 Aug	0.60	365	Max pcorr	Linear	-
3	1 Jun-31 Aug	0.67	365	Max pcorr	Linear	-
4	1 Jun-31 Aug	0.75	365	Max pcorr	Linear	-
5	1 Jun-31 Aug	0.80	365	Max pcorr	Linear	-
6	1 Jun-31 Aug	0.90	365	Max pcorr	Linear	-
7	15 Jun-31 Jul (peak)	0.50	365	Max pcorr	Linear	-
8	15 Jun-31 Jul (peak)	0.60	365	Max pcorr	Linear	-
9	15 Jun-31 Jul (peak)	0.67	365	Max pcorr	Linear	-
10	15 Jun-31 Jul (peak)	0.75	365	Max pcorr	Linear	-
11	15 Jun-31 Jul (peak)	0.80	365	Max pcorr	Linear	-
12	15 Jun-31 Jul (peak)	0.90	365	Max pcorr	Linear	-
13	1 Jun-31 Aug	0.67	240	Max pcorr	Linear	-
14	1 Jun-31 Aug	0.67	120	Max pcorr	Linear	-
15	1 Jun-31 Aug	0.67	365	Mean pcorr	Linear	-
16	2 Jun-31 Aug	0.67	365	Max pcorr	Quadratic	-
17	5 Jun-31 Aug	0.67	365	Max pcorr	Month FE	-
18	1 Jun-31 Aug	0.67	365	Total communicability	Linear	0.25
19	1 Jun-31 Aug	0.67	365	Total communicability	Linear	0.50
20	1 Jun-31 Aug	0.67	365	Total communicability	Linear	1.00
21	1 Jun-31 Aug	0.67	365	Total communicability	Linear	2.00

Table 5.2. Specification grid for DiD estimations

Each specification corresponds to a difference-in-differences estimation using the Callaway-Sant'Anna estimator (Callaway and Sant'Anna 2021). "Threshold" defines the quantile threshold for High category assignment based on pre-drought network exposure. "Max/Mean pcorr" denote the aggregation method for partial correlations to anchor baskets. Alternative detrending procedures include polynomial detrending and month fixed effects. The total communicability parameter β defines the relative weight on network walk length: smaller β emphasizes direct links, while larger β incorporates longer indirect paths.

The 2012 summer drought induced statistically significant and economically meaningful increases in contemporaneous partial correlations that are unmatched elsewhere in the 2006–2023 sample. For the corn–wheat anchor basket (Figure 5.7), 16 of 21 specifications yield positive and statistically significant treatment effects, with baseline partial-correlation estimates ranging from 0.006 to 0.036 and the highest total communicability specification ($\beta = 2.00$) reaching 0.128. The soybean complex (Figure 5.8) displays nearly identical robustness, with 17 of 21 specifications significant and positive. Baseline estimates cluster tightly, while communicability-based measures produce amplified effects. The consistency across both anchor configurations - one centered on corn–wheat substitution and the other on the soybean processing chain - indicates that the observed tightening reflects localized supply disruption rather than specification sensitivity or spurious correlation.

No other year in the sample approaches 2012's consistency of positive and significant effects. The 2006–2008 period shows limited and unstable positive estimates, while the 2008

financial crisis itself is characterized by near-zero effects, consistent with contemporaneous fragmentation under fast-breaking shocks. The 2009–2011 commodity boom produces predominantly negative estimates, indicating network contraction rather than clustering.

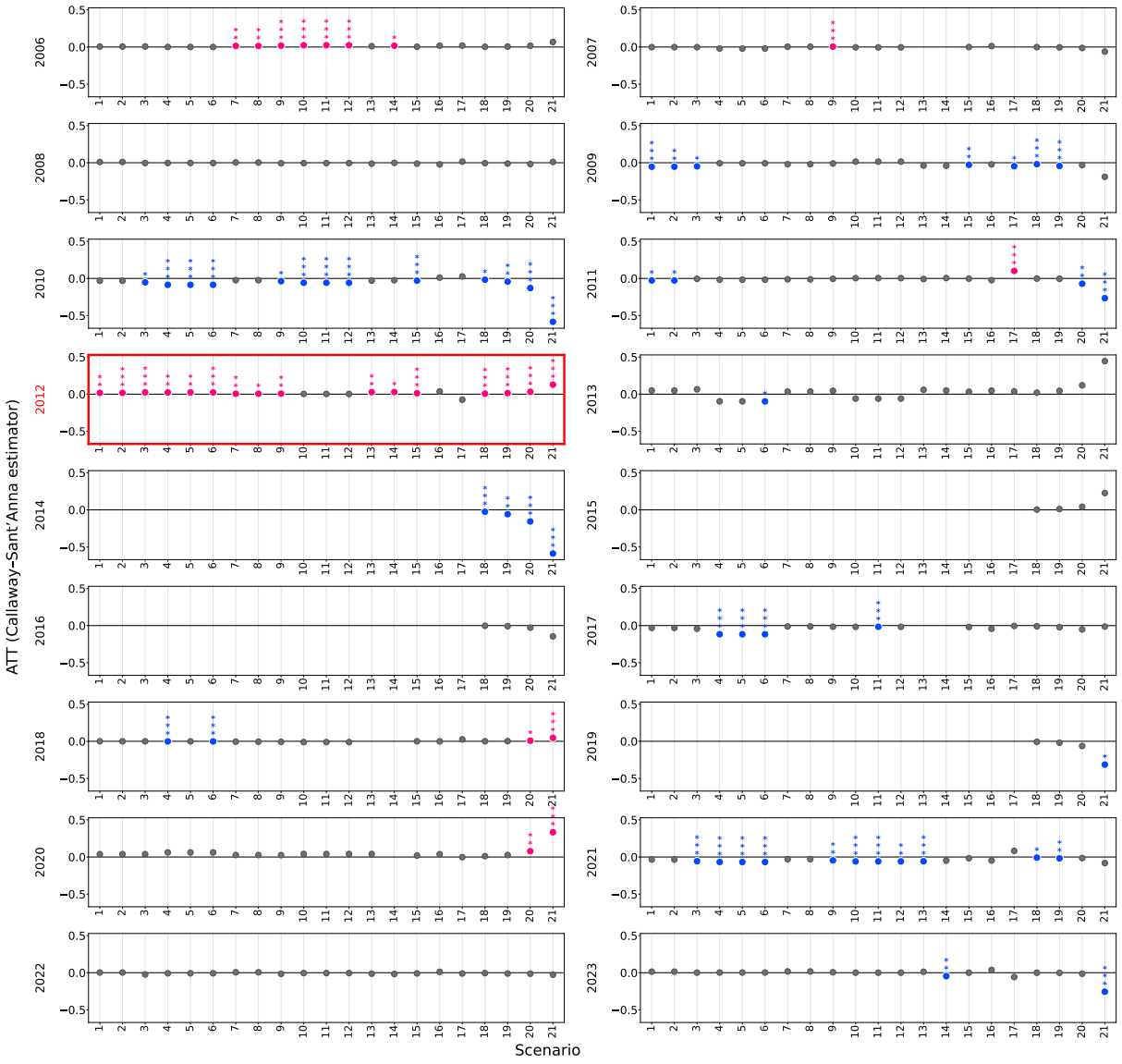


Figure 5.7. Corn and Wheat

Difference-in-differences estimates of drought impact on network contemporaneous connectivity: corn-wheat anchor basket, 2006-2023. Each panel displays ATT estimates for a given year across 21 robustness specifications (Table 5.2). Significance levels: * $p < 0.10$, ** $p < 0.05$, *** $p < 0.01$.

Post-2012 years likewise fail to exhibit systematic tightening. In particular, the widely discussed 2021 drought generates fragmentation (negative estimates) for the corn–wheat anchor and only modest, unstable effects for the soybean complex. This divergence reflects its weaker geographic overlap with core Midwest production and limited realized yield losses (the expectation of losses did not materialize and yields were good), which constrained systemic propagation despite localized stress (S. Irwin 2023a; S. Irwin 2023b; USDA NASS 2026a; USDA NASS 2026b). The 2022–2023 Western drought episodes,

concentrated outside central production regions, similarly do not induce broad network reorganization.

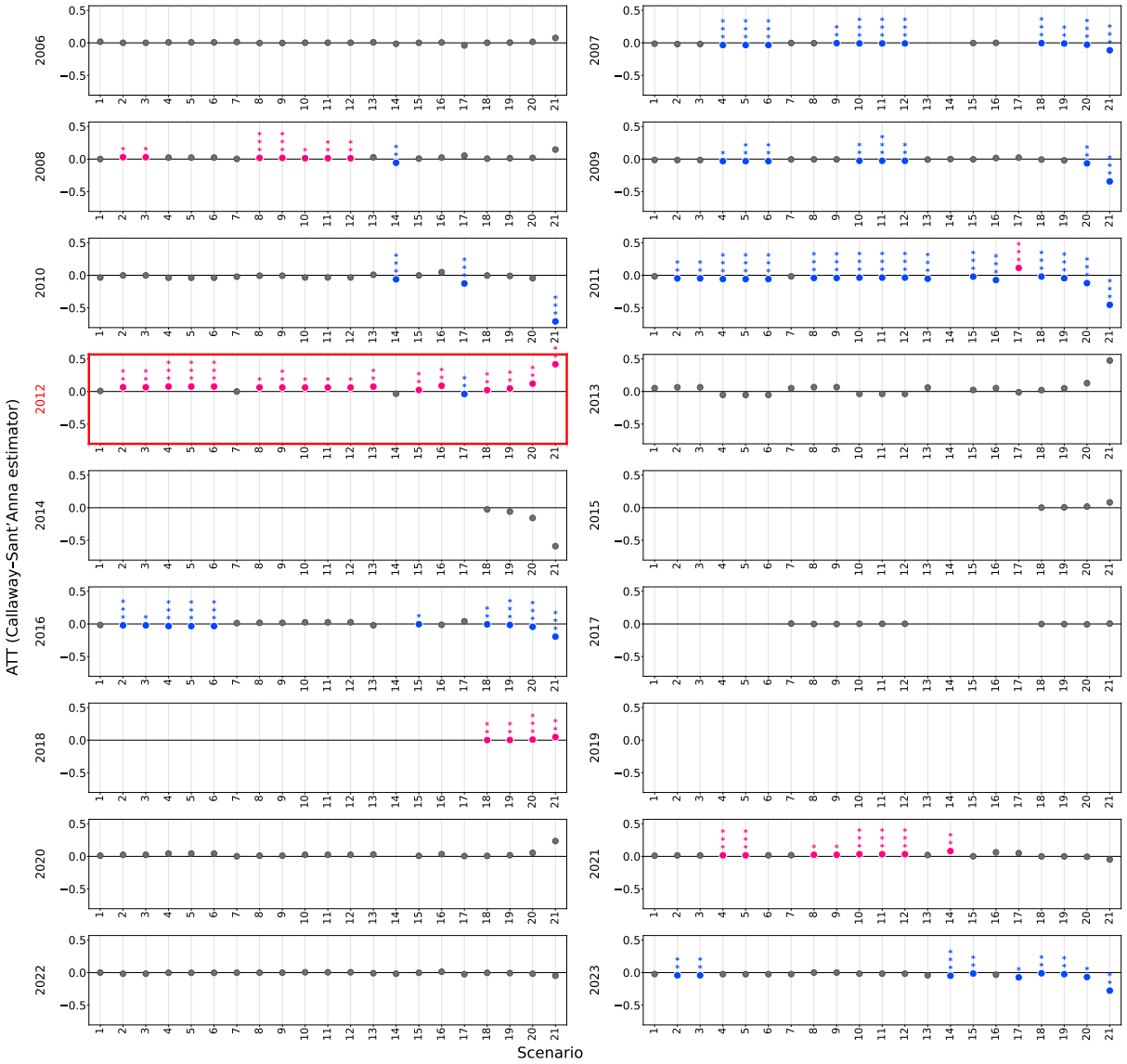


Figure 5.8. Soybeans, Soybean Oil and Soybean Meal

Difference-in-differences estimates of drought impact on network contemporaneous connectivity: corn-wheat anchor basket, 2006-2023. Each panel displays ATT estimates for a given year across 21 robustness specifications (Table 5.2). Significance levels: * $p < 0.10$, ** $p < 0.05$, *** $p < 0.01$.

The specification grid (Table 5.2) addresses potential identification concerns by varying the exposure threshold, event window, pre-period length, aggregation rule, and detrending procedure. For 2012, treatment effects remain positive across conservative and permissive threshold choices and are robust to alternative pre-window lengths. Restricting the event window to the peak drought period attenuates magnitudes but preserves the positive sign, consistent with gradual information accumulation. In contrast, applying the same peak-window design to non-core drought years such as 2021 yields negative or unstable effects, indicating that timing sensitivity reflects genuine agronomic exposure rather than

mechanical window selection.

Alternative exposure mappings and detrending procedures further clarify the mechanism. Using mean instead of maximum partial correlations reduces magnitudes but preserves statistical significance, suggesting that reorganization concentrates in contracts' strongest anchor link. Quadratic detrending delivers similar results, while month fixed effects absorb much of the summer tightening, consistent with seasonal collinearity. Total communicability specifications amplify the magnitude of the 2012 effects, particularly at higher β, but do not produce comparable positive and significant results in other years. This pattern suggests that long-path aggregation strengthens measured clustering during the drought without generating false positives elsewhere, while baseline partial-correlation measures remain more directly interpretable in economic terms.

These findings validate our framework distinguishing slow-building from fast-breaking shocks. The 2012 drought unfolded gradually through sequential USDA crop condition reports: for June 10, 2012, 54% of the corn crop was rated "Good" and 12% "Excellent" (USDA, NASS 2012a), while the July 22 report confirmed catastrophic damage - 23% "Good" with a mere 3% rated "Excellent" (USDA, NASS 2012b). Our DiD window (June 1-August 31) captures this accumulation phase, during which market participants continuously revised beliefs, rebalanced hedges, and adjusted substitution strategies. The network's response (sustained tightening of contemporaneous dependencies without corresponding predictive spillover increases, see Granger results in Figures 5 and 6 in Appendix 3) aligns precisely with the information aggregation and portfolio (hedging positions, hedge ratios) rebalancing strategies: as drought severity became apparent, corn and soybeans became joint proxies for Midwest agricultural conditions, elevating their partial correlations with substitutes and downstream products while information efficiency prevented persistent lead-lag patterns in daily data. Consistent with this interpretation, Granger predictability remains muted during the slow-building drought window because price discovery operates contemporaneously at daily frequency; in contrast, discrete announcement events (Table 3 in Appendix 1) generate short-lived Granger spikes reflecting temporary asynchronous adjustment across contracts, rather than persistent transmission mechanisms.

The cross-year comparison underscores information arrival speed's centrality to propagation dynamics. Fast shocks such as the September 2008 Lehman collapse or July 2013 JPMorgan commodity exit trigger immediate volatility spikes and network fragmentation

(Lautier, Ling, and Raynaud 2015), visible as contemporaneous decoupling rather than clustering (Figure 5.5). Weather events outside core production regions (2021-2022 Western drought, 2017-2018 Plains drought) lack sufficient exposure to central network nodes, failing to reorganize systemic dependencies despite localized price impacts. Only the 2012 Midwest drought combined gradual information revelation, catastrophic magnitude (>$26 billion damage, EM-DAT: The International Disaster Database 2024), precise geographic overlap with corn/soybean centrality, and timing aligned with critical yield-formation windows, generating conditions for slow-shock amplification through network structure. In sum, 2012's exceptional robustness across standard specifications (16 of 21 significant positive for corn-wheat, 17 of 21 for soybeans) distinguishes it from all comparison years.[13]

6. Conclusion

We reconstruct the time-varying network structure of ten agricultural futures over twenty years (2004–2024) using the Sparse VAR Network Estimation (NETS) methodology of Barigozzi and Brownlees (2019), and we show that agricultural commodities organize into distinct grain and soft clusters, where corn and soybeans emerge as central nodes. We document that discrete financial shocks trigger immediate network fragmentation and spikes in predictive spillovers. In contrast, applying a novel network difference-in-differences design to the 2012 U.S. drought reveals that this slow-building physical shock induced a statistically significant structural densification, tightening contemporaneous linkages around the market's central grain core.

This paper examines whether the speed of information arrival determines the topology of financial contagion. Our findings offer two specific contributions to the literature on systemic risk and financial networks. First, we empirically distinguish between slow and fast systemic risk by demonstrating that the temporal structure of uncertainty resolution might change network topology. Because gradual physical shocks provide the latency necessary for sequential substitution arbitrage and the cross-hedging of anticipated physical adaptations, these mechanisms actively tighten contemporaneous network linkages rather than inducing the fragmentation seen during abrupt financial surprises. Second, we methodologically advance the literature by introducing a network causal inference (difference-in-differences) design that overcomes the endogeneity of simultaneous topological rewiring by assigning

[13]For transparency, we complement the DiD estimates of Callaway and Sant'Anna (2021) with a simple calendar-time 2×2 DiD computed on the High-Low difference series, $D_t \equiv \tilde{\bar{Y}}_{\text{High},t} - \tilde{\bar{Y}}_{\text{Low},t}$ (Figure 7 in Appendix 3). See details in Appendix 3.

treatment via ex-ante exposure to an exogenous physical shock.

Our analysis has several limitations. First, we focus on U.S. agricultural futures, which serve as global benchmarks but may not fully capture substitution dynamics in local physical markets. Second, the use of daily data captures inter-day network reorganization but cannot resolve intra-day liquidity adjustments. Future research could extend this framework to other slow-moving climate shocks or sequential regulatory events where information unfolds gradually over time.

Ultimately, our findings provide a new perspective on the foundations of static risk management. Standard diversification logic implicitly treats correlation structures as exogenous or slow-moving, assuming that idiosyncratic physical shocks will not systematically reorganize market dependence. We document the opposite for slow-building climate shocks: as uncertainty accumulates, the network's contemporaneous conditional dependence tightens endogenously around central contracts, weakening diversification precisely when it is most relied upon. This distinction between fast fragmentation and slow clustering suggests that systemic risk is not determined solely by shock magnitude, but by the temporal structure of information arrival. When shocks unfold gradually, markets adapt in ways that amplify comovement through existing substitution and hedging channels. Recognizing this endogenous rewiring of financial networks is essential for advancing research on futures pricing, and the dynamic measurement of systemic exposure.

Bibliography

Acemoglu, Daron, Asuman Ozdaglar, and Alireza Tahbaz-Salehi (2015). "Systemic Risk and Stability in Financial Networks". In: *American Economic Review* 105.2, pp. 564–608.

Acharya, Viral, Robert Engle, and Matthew Richardson (2012). "Capital shortfall: A new approach to ranking and regulating systemic risks". In: *American Economic Review* 102.3, pp. 59–64. DOI: 10.1257/aer.102.3.59.

Acharya, Viral V., Lars A. Lochstoer, and Tarun Ramadorai (2013). "Limits to Arbitrage and Hedging: Evidence from Commodity Markets". In: *Journal of Financial Economics* 109.2, pp. 441–465.

Adjemian, Michael K. (2012). "Quantifying the WASDE Announcement Effect". In: *American Journal of Agricultural Economics* 94.1, pp. 238–256.

Adrian, Tobias and Markus K Brunnermeier (2011). *CoVaR*. Tech. rep. National Bureau of Economic Research. DOI: 10.3386/w17454.

Arkhangelsky, Dmitry et al. (2021). "Synthetic Difference-in-Differences". In: *American Economic Review* 111.12, pp. 4088–4118.

Aulerich, Nicole M., Scott H. Irwin, and Philip Garcia (2014). "Bubbles, Food Prices, and Speculation: Evidence from the CFTC's Daily Large Trader Data Files". In: *The Economics of Food Price Volatility*. Ed. by Jean-Paul Chavas, David Hummels, and Brian Wright. Chicago: University of Chicago Press, pp. 211–253.

Autor, David H., William R. Kerr, and Adriana D. Kugler (2007). "Does Employment Protection Reduce Productivity? Evidence from US States". In: *The Economic Journal* 117.521, F189–F217.

Barigozzi, Matteo and Christian Brownlees (2019). "Nets: Network estimation for time series". In: *Journal of Applied Econometrics* 34.3, pp. 347–364. DOI: https://doi.org/10.1002/jae.2676.

Basak, Suleyman and Anna Pavlova (2016). "A model of financialization of commodities". In: *The Journal of Finance* 71.4, pp. 1511–1556. DOI: https://doi.org/10.1111/jofi.12408.

Benzi, Michele and Christine Klymko (2013). "Total communicability as a centrality measure". In: *Journal of Complex Networks* 1.2, pp. 124–149.

Bhar, Ramaprasad and AG Malliaris (2011). "Oil prices and the impact of the financial crisis of 2007–2009". In: *Energy Economics* 33.6, pp. 1049–1054. DOI: https://doi.org/10.1016/j.eneco.2011.01.016.

Bianchi, Robert J, John Hua Fan, and Neda Todorova (2020). "Financialization and de-financialization of commodity futures: A quantile regression approach". In: *International Review of Financial Analysis* 68, p. 101451. DOI: https://doi.org/10.1016/j.irfa.2019.101451.

Bisias, Dimitrios et al. (2012). "A Survey of Systemic Risk Analytics". In: *Annual Review of Financial Economics* 4.1, pp. 255–296.

Bouri, Elie et al. (2021). "The realized volatility of commodity futures: Interconnectedness and determinants". In: *International Review of Economics & Finance* 73, pp. 139–151. DOI: https://doi.org/10.1016/j.iref.2021.01.006.

Brunnermeier, Markus K. and Lasse Heje Pedersen (2009). "Market Liquidity and Funding Liquidity". In: *Review of Financial Studies* 22.6, pp. 2201–2238.

Büyükşahin, Bahattin and Michel A. Robe (May 2024). "Does "Paper Oil" Matter? Energy Markets' Financialization and Co-Movements with Equity Markets". In: *Commodities* 3.2, pp. 1–28. DOI: https://doi.org/10.3390/commodities3020013.

Bykhovskaya, Anna (2022). "Time series approach to the evolution of networks: Prediction and estimation". In: *Journal of Business & Economic Statistics* 41.1, pp. 170–183. DOI: https://doi.org/10.1080/07350015.2021.2006669.

Callaway, Brantly and Pedro H. C. Sant'Anna (2021). "Difference-in-differences with multiple time periods". In: *Journal of Econometrics* 225.2, pp. 200–230.

Cao, A. N. and Michel A. Robe (2022). "Market Uncertainty and Sentiment Around USDA Announcements". In: *Journal of Futures Markets* 42.2, pp. 250–275.

Cao, Yan, Sheng Cheng, and Xinran Li (2024). "Co-movements between heterogeneous crude oil and food markets: Does temperature change really matter?" In: *Research in International Business and Finance* 67, p. 102113. DOI: https://doi.org/10.1016/j.ribaf.2023.102113.

Cheng, Ing-Haw, Andrei Kirilenko, and Wei Xiong (2015). "Convective Risk Flows in Commodity Futures Markets". In: *Review of Finance* 19.5, pp. 1733–1781.

Cheng, Ing-Haw and Wei Xiong (2014). "Financialization of Commodity Markets". In: *Annual Review of Financial Economics* 6.1, pp. 419–441.

CME Group (2025). *Understanding Soybean Crush*. https://www.cmegroup.com/education/courses/introduction-to-agriculture/grains-oilseeds/understanding-soybean-crush.html. CME Institute, educational module on Soybean Crush trading and calculation.

EM-DAT: The International Disaster Database (2024). *EM-DAT: The International Disaster Database*. https://www.emdat.be.

De Winne, Jasmien and Gert Peersman (2021). "The adverse consequences of global harvest and weather disruptions on economic activity". In: *Nature Climate Change* 11.8, pp. 665–672. DOI: https://doi.org/10.1038/s41558-021-01102-w.

Diebold, Francis X and Kamil Yilmaz (2012). "Better to give than to receive: Predictive directional measurement of volatility spillovers". In: *International Journal of forecasting* 28.1, pp. 57–66. DOI: https://doi.org/10.1016/j.ijforecast.2011.02.006.

Diebold, Francis X and Kamil Yilmaz (2014). "On the network topology of variance decompositions: Measuring the connectedness of financial firms". In: *Journal of econometrics* 182.1, pp. 119–134. DOI: https://doi.org/10.1016/j.jeconom.2014.04.012.

Duarte, Fernando and Thomas M. Eisenbach (2021). "Fire-Sale Spillovers and Systemic Risk". In: *The Journal of Finance* 76.3, pp. 1251–1294.

Dube, Arindrajit, T. William Lester, and Michael Reich (2010). "Minimum Wage Effects across State Borders: Estimates Using Contiguous Counties". In: *The Review of Economics and Statistics* 92.4, pp. 945–964.

Duffie, Darrell (2010). "Presidential address: Asset price dynamics with slow-moving capital". In: *The Journal of Finance* 65.4, pp. 1237–1267.

Ekeland, Ivar, Delphine Lautier, and Bertrand Villeneuve (2019). "Hedging pressure and speculation in commodity markets". In: *Economic Theory* 68, pp. 83–123. DOI: https://doi.org/10.1007/s00199-018-1115-y.

Elliott, Matthew, Benjamin Golub, and Matthew O. Jackson (2014). "Financial Networks and Contagion". In: *American Economic Review* 104.10, pp. 3115–3153.

Engle, Robert and Bryan Kelly (2012). "Dynamic equicorrelation". In: *Journal of Business & Economic Statistics* 30.2, pp. 212–228. DOI: https://doi.org/10.1080/07350015.2011.652048.

Estrada, Ernesto and Naomichi Hatano (2008). "Communicability in complex networks". In: *Physical Review E* 77.3, p. 036111. DOI: 10.1103/PhysRevE.77.036111.

Fama, Eugene F. (1965). "The Behavior of Stock-Market Prices". In: *The Journal of Business* 38.1, pp. 34–105.

Fama, Eugene F. and Kenneth R. French (1987). "Commodity Futures Prices: Some Evidence on Forecast Power, Premiums, and the Theory of Storage". In: *The Journal of Business* 60.1, pp. 55–73. DOI: http://www.jstor.org/stable/2352947.

Freyaldenhoven, Simon, Christian Hansen, and Jesse M. Shapiro (2019). "Pre-Event Trends in the Panel Event-Study Design". In: *American Economic Review* 109.9, pp. 3307–3338.

Fruchterman, Thomas M. J. and Edward M. Reingold (1991). "Graph Drawing by Force-Directed Placement". In: *Software: Practice and Experience* 21.11, pp. 1129–1164. DOI: 10.1002/spe.4380211102.

Garcia, Philip, Scott H. Irwin, and Aaron Smith (2015). "Futures Market Failure?" In: *American Journal of Agricultural Economics* 97.1, pp. 40–64.

Goldstein, Itay and Liyan Yang (2022). "Commodity Financialization and Information Transmission". In: *The Journal of Finance* 77.5, pp. 2613–2667.

Guo, Kun et al. (2023). "How are climate risk shocks connected to agricultural markets?" In: *Journal of Commodity Markets* 32, p. 100367. DOI: https://doi.org/10.1016/j.jcomm.2023.100367.

Irwin, Scott (2023a). "The Relative Impact of Crop Weather Variables on the US Average Yield of Corn". In: *farmdoc daily* 13.184.

— (2023b). "The Relative Impact of Crop Weather Variables on the US Average Yield of Soybeans". In: *farmdoc daily* 13.194.

Jetsupphasuk, Michael, Didong Li, and Michael G. Hudgens (2025). "Estimating causal effects using difference-in-differences under network dependency and interference". In: *arXiv preprint*. arXiv: 2502.03414.

Kang, Sang Hoon, Ron McIver, and Seong-Min Yoon (2017). "Dynamic spillover effects among crude oil, precious metal, and agricultural commodity futures markets". In: *Energy Economics* 62, pp. 19–32. DOI: https://doi.org/10.1016/j.eneco.2016.12.011.

Kang, Sang Hoon, Aviral Kumar Tiwari, et al. (2019). "Exploring the time-frequency connectedness and network among crude oil and agriculture commodities V1". In: *Energy Economics* 84, p. 104543. DOI: https://doi.org/10.1016/j.eneco.2019.104543.

Kang, Wenjin, K Geert Rouwenhorst, and Ke Tang (2020). "A tale of two premiums: The role of hedgers and speculators in commodity futures markets". In: *The Journal of Finance* 75.1, pp. 377–417. DOI: https://doi.org/10.1111/jofi.12845.

Kang, Wenjin, Ke Tang, and Ningli Wang (2023). "Financialization of commodity markets ten years later". In: *Journal of Commodity Markets* 30, p. 100313. DOI: https://doi.org/10.1016/j.jcomm.2023.100313.

Khalfaoui, Rabeh et al. (2021). "Connectedness between energy and nonenergy commodity markets: Evidence from quantile coherency networks". In: *Resources Policy* 74, p. 102318. DOI: https://doi.org/10.1016/j.resourpol.2021.102318.

Lark, Tyler J et al. (2022). "Environmental outcomes of the US renewable fuel standard". In: *Proceedings of the National Academy of Sciences* 119.9, e2101084119. DOI: https://doi.org/10.1073/pnas.2101084119.

Lautier, Delphine, Julien Ling, and Franck Raynaud (2015). *Integration of commodity derivative markets: Has it gone too far?* Springer. DOI: https://doi.org/10.1007/978-1-4939-2733-3_3.

Lautier, Delphine and Franck Raynaud (2012). "Systemic risk in energy derivative markets: a graph-theory analysis". In: *The Energy Journal* 33.3, pp. 215–240. DOI: https://doi.org/10.5547/01956574.33.3.8.

Lee, Seongho (2025). "Field-Level Crop Choice Responses to Weather-Induced Yield Shocks in the US Corn Belt". In: *American Journal of Agricultural Economics*.

Lee, Soo Jeong and Jeffrey M. Wooldridge (2023). "A Simple Transformation Approach to Difference-in-Differences Estimation for Panel Data". Available at SSRN: https://papers.ssrn.com/sol3/papers.cfm?abstract_id=4516518.

Letta, Marco, Pierluigi Montalbano, and Guillaume Pierre (2022). "Weather shocks, traders' expectations, and food prices". In: *American Journal of Agricultural Economics* 104.3, pp. 1100–1119. DOI: https://doi.org/10.1111/ajae.12258.

Liu, Cheng and Yixiao Sun (2019). "A Simple and Trustworthy Asymptotic t Test in Difference-in-Differences Regressions". In: *Journal of Econometrics* 210.2, pp. 327–362. DOI: 10.1016/j.jeconom.2019.02.003.

Makkonen, Adam et al. (2021). "The effect of temperature anomaly and macroeconomic fundamentals on agricultural commodity futures returns". In: *Energy Economics* 100, p. 105377. DOI: https://doi.org/10.1016/j.eneco.2021.105377.

Mantegna, Rosario N (1999). "Hierarchical structure in financial markets". In: *The European Physical Journal B-Condensed Matter and Complex Systems* 11, pp. 193–197. DOI: https://doi.org/10.1007/s100510050929.

Mitchell, Mark, Lasse H. Pedersen, and Todd Pulvino (2007). "Slow moving capital". In: *American Economic Review* 97.2, pp. 215–220.

Mlikota, Marko (2023). *Cross-sectional dynamics under network structure: Theory and macroeconomic applications*. Verlag nicht ermittelbar.

Morgan, J.P. (2024). *Cocoa Prices*. Accessed: 2024-06-05. URL: https://www.jpmorgan.com/insights/global-research/commodities/cocoa-prices.

OECD and Food and Agriculture Organization of the United Nations (2018). *OECD-FAO Agricultural Outlook 2018–2027, Chapter 5: Sugar*. https://www.fao.org/4/i9166e/i9166e_Chapter5_Sugar.pdf. p. 143.

Paris, Anthony (2018). "On the link between oil and agricultural commodity prices: Do biofuels matter?" In: *International Economics* 155, pp. 48–60. DOI: https://doi.org/10.1016/j.inteco.2017.12.003.

Peng, Kexin et al. (2021). *Canary in the Coal Mine: COVID-19 and Soybean Futures Market Liquidity*. https://ssrn.com/abstract=3780322. Available at SSRN 3780322.

Reuters (July 26, 2013). *Under siege, JPMorgan to quit physical commodities*. Accessed: 2025-07-15. Reuters. URL: https://www.reuters.com/article/business/under-siege-jpmorgan-to-quit-physical-commodities-idUSBRE96P10M/.

Roth, Jonathan et al. (2023). "What's Trending in Difference-in-Differences? A Synthesis of the Recent Econometrics Literature". In: *Journal of Econometrics* 235.2, pp. 2218–2244.

Saghaian, Sayed et al. (2018). "Asymmetric price volatility transmission between US biofuel, corn, and oil markets". In: *Journal of Agricultural and Resource Economics*, pp. 46–60. DOI: https://www.jstor.org/stable/44840974.

Sanders, Dwight R., Scott H. Irwin, and Richard P. Merrin (2010). "The Adequacy of Speculation in Agricultural Futures Markets: Too Much of a Good Thing?" In: *Applied Economic Perspectives and Policy* 32.1, pp. 77–94.

Shahzad, Farrukh et al. (2021). "Energy, agriculture, and precious metals: Evidence from time-varying Granger causal relationships for both return and volatility". In: *Resources Policy* 74, p. 102298. DOI: https://doi.org/10.1016/j.resourpol.2021.102298.

Taşkin, Dilvin, Efe Caglar Cagli, and Pınar Evrim Mandaci (2021). "The impact of temperature anomalies on commodity futures". In: *Energy Sources, Part B: Economics, Planning, and Policy* 16.4, pp. 357–370. DOI: https://doi.org/10.1080/15567249.2021.1922546.

U.S. Department of Agriculture, Economic Research Service (2024). *Soybeans and Oil Crops: Related Data & Statistics*. URL: https://www.ers.usda.gov/topics/crops/soybeans-and-oil-crops/related-data-statistics/.

U.S. Department of Agriculture, Foreign Agricultural Service (July 2025). *Production – Soybeans (Commodity 2222000)*. https://www.fas.usda.gov/data/production/commodity/2222000. Production Supply and Distribution (PSD) data.

U.S. Department of Agriculture, Office of the Chief Economist (July 2025). *World Agricultural Supply and Demand Estimates (WASDE-662), July 11, 2025*. https://www.usda.gov/oce/commodity/wasde/wasde0725.pdf. Approved by the World Agricultural Outlook Board; ISSN 1554-9089.

United Soybean Board (2024). *Biodiesel: Soybean Oil's Contribution to The U.S. Economy*. URL: https://www.unitedsoybean.org/issue-briefs/biodiesel/.

USDA NASS (2026a). *Corn Yield*. USDA NASS. URL: https://www.nass.usda.gov/Charts_and_Maps/Field_Crops/cornyld.php (visited on 01/14/2026).

— (2026b). *Soybeans Yield*. USDA NASS. URL: https://www.nass.usda.gov/Charts_and_Maps/Field_Crops/soyyld.php (visited on 01/14/2026).

USDA, NASS (June 11, 2012a). *Crop Progress*. Statistical Release ISSN 1948-3007. Washington, DC: USDA, Agricultural Statistics Board.

— (July 23, 2012b). *Crop Progress*. Statistical Release ISSN 1948-3007. Washington, DC: USDA, Agricultural Statistics Board.

Vives, Xavier (2008). "Innovation and competitive pressure". In: *The Journal of Industrial Economics* 56.3, pp. 419–469.

Wang, Junxian et al. (2020). "Effects of replacing soybean meal with cottonseed meal on growth, feed utilization and non-specific immune enzyme activities for juvenile white shrimp, *Litopenaeus vannamei*". In: *Aquaculture Reports* 16, p. 100255. DOI: 10.1016/j.aqrep.2019.100255.

Xiao, Binqing et al. (2020). "Estimating the connectedness of commodity futures using a network approach". In: *Journal of Futures Markets* 40.4, pp. 598–616. DOI: https://doi.org/10.1002/fut.22086.

Zhang, Dongna et al. (2023). “Impacts of weather conditions on the US commodity markets systemic interdependence across multi-timescales”. In: *Energy Economics* 123, p. 106732. DOI: https://doi.org/10.1016/j.eneco.2023.106732.

Appendix

1 Data

Commodity	Code	Exchange	Vol (1)	Commodity	Code	Exchange	Vol (1)
Grains				**Softs**			
Corn	C	CBoT	108,451.0	Coffee	KC	ICE-US	10,456.3
Wheat	W	CBoT	40,449.4	Cocoa US	CC	ICE-US	9,719.5
Soybeans	S	CBoT	62,384.9	Cocoa UK	LCC	ICE London	5,425.1
Soybean Meal	SM	CBoT	23,924.9	Sugar	SB	ICE-US	49,464.9
Soybean Oil	BO	CBoT	27,010.7	Cotton	CT	ICE-US	9,036.4

Table 1. Commodity contracts and first-maturity trading volumes

Contract	Country of Origin	Used for energy
Grains		
Corn CBoT	US	Yes
Soybeans CBoT	US	Yes
Soybean Oil CBoT	US	Yes
Soybean Meal CBoT	US	No
Wheat CBoT	US	No
Softs		
Coffee ICE-US (Arabica)	Mexico, Salvador, Guatemala, Costa Rica, Nicaragua, Kenya, Papua New Guinea, Panama, Tanzania, Uganda, Honduras, Peru, Colombia, Burundi, Rwanda, Venezuela, India, Dominican Republic, Ecuador, Brazil	No
Cocoa ICE-US	Ghana, Ivory Coast, Nigeria, Sierra Leone, Togo, Ecuador, Cameroon, Colombia, New Guinea, Venezuela, Bolivia, Haiti, Indonesia-Sulawesi, Malaysia	No
London Cocoa ICE	African and other origins	No
Sugar ICE-US No.11	Argentina, Australia, Barbados, Belize, Brazil, Colombia, Costa Rica, Dominican Republic, El Salvador, Ecuador, Fiji Islands, Guatemala, Honduras, India, Jamaica, Malawi, Mauritius, Mexico, Mozambique, Nicaragua, Peru, Republic of the Philippines, South Africa, Swaziland, Taiwan, Thailand, Trinidad, United States, Zimbabwe	Yes
Cotton ICE-US No.2	US	No

Table 2. Origins of commodity futures contracts

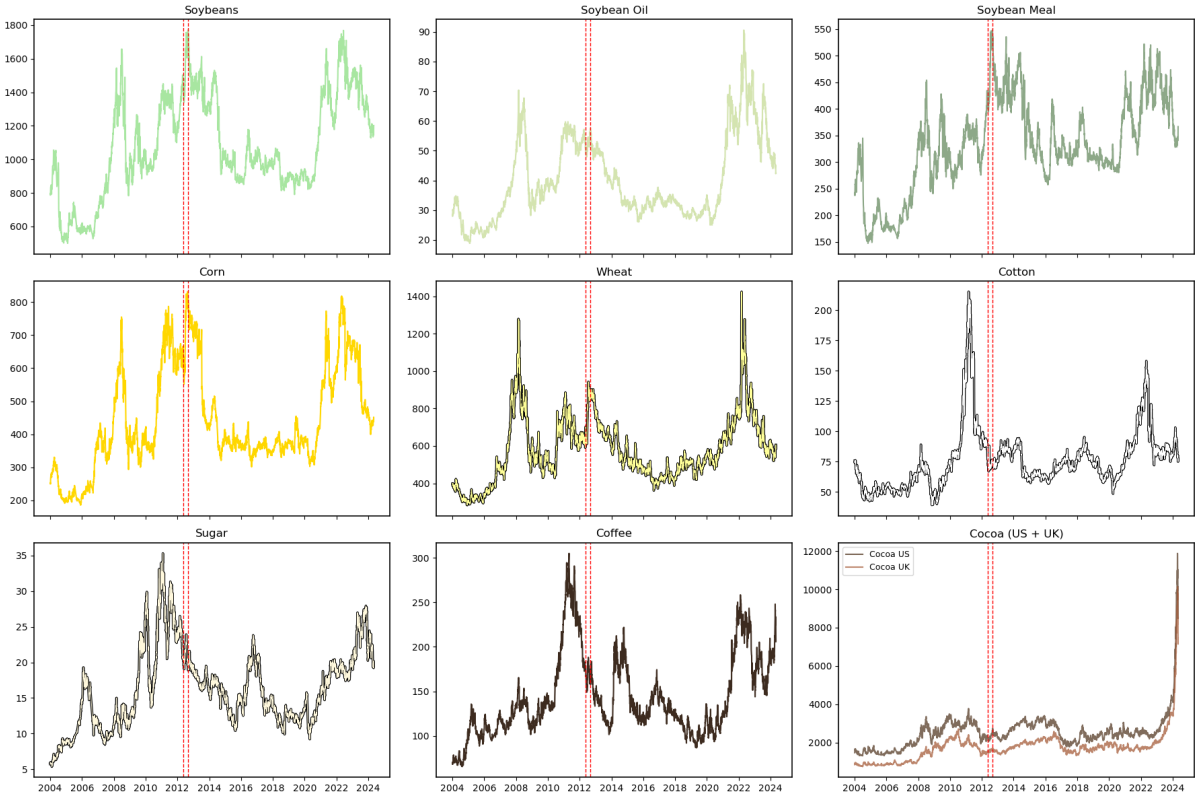


Figure 1. Price evolution with 2012 drought period indicators

Date	Event & Shock Topology	Description
19 Dec 2007	**U.S. Ethanol Mandate (EISA)** *Structural Policy Shock (Slow-Building)*	The US Renewable Fuel Standard (RFS) was launched during that period and it is the world's largest biofuel program, creating a permanent structural bridge between energy and agricultural clusters. This program sets the minimum volume of biofuels such as ethanol that must be used each year for transportation fuel. Lark et al. (2022) find that RFS raised Corn prices by 30% and the prices of other crops increased by 20% in the years after the introduction of the policy (2008 to 2016). In addition to Corn price increases, the demand for biofuels also rose during that period as GFC provoked a sharp increase in oil prices that peaked in June 2008 at 133 dollars before falling to 39 dollars in February 2009 (Bhar and Malliaris 2011).
15 Sep 2008	**Lehman Brothers Collapse** *Financial Liquidity Shock (Fast/Systemic)*	The bankruptcy triggered a global liquidity crisis, forcing simultaneous cross-asset liquidations. This event caused a massive spike in volatility spillovers from equities to commodities as financial intermediaries withdrew arbitrage capital, overriding physical fundamentals and generating a "predictive spike" in the network (Diebold and Yilmaz 2012; S. H. Kang, McIver, and Yoon 2017).
15 Aug 2010	**Russian Grain Export Ban** *Geopolitical Supply Shock (Fast/Discrete)*	Russia announced a sudden export ban following heatwaves. Unlike the gradual pricing of weather risk, the announcement acted as a discrete supply shock, triggering immediate global repricing and a sharp spike in predictive spillovers (De Winne and Peersman 2021).
01 Jun 2012 - 01 Sep 2012	**U.S. Midwest Drought** *Physical Climate Shock (Slow/Sequential)*	A severe drought where information was revealed sequentially through weekly USDA crop condition reports rather than a single announcement. This allowed market participants to gradually rebalance hedges and substitute feed inputs, resulting in a "slow-motion" tightening of network interconnectedness rather than a liquidity-driven spike.
26 Jul 2013	**JPMorgan Exits Commodities** *Regulatory Structural Shock (Fast/Discrete)*	JPMorgan announced its exit from physical commodity trading amidst regulatory pressure. This event marked the onset of "de-financialization," reducing institutional participation and liquidity. It triggered a structural break in the network, weakening the financial-commodity link and reducing the contemporaneous dependence of the system (Bianchi, Fan, and Todorova 2020).

Date	Event & Shock Topology	Description
07 Aug 2014	**Russian Food Import Ban** *Geopolitical Trade Shock (Fast/Discrete)*	Retaliatory ban on Western food imports. This event acted as a structural break that severed specific trade links, forcing immediate reallocation of flows and altering the volatility transmission network for dairy and meat products (Guo et al. 2023).
20 Apr 2020	**WTI Turns Negative** *Financial Friction (Fast/Liquidity Crisis)*	WTI futures fell to −$37.63 due to storage constraints and ETF "Trading-at-Settlement" mechanisms. Unlike the drought, this financialized shock triggered a massive spike in predictive linkages without contemporaneous decoupling, as index funds forced correlations to remain high despite the crash (W. Kang, Tang, and N. Wang 2023).
24 Feb 2022 - now	**Russia–Ukraine War** *Geopolitical War Shock (Fast/Systemic)*	The invasion disrupted global exports of grain, fertilizer, and energy simultaneously. This constituted a systemic supply shock that pushed total volatility spillovers to historical highs, synchronizing price movements across the entire commodity complex.

Table 3. Commodity Market Events and Structural Shock Classification

2 Methodology

2.1 Alternative Detrending Procedures

We use alternative (non linear) detrending operators in the DiD analysis for two specifications. All detrending is performed separately for each candidate year y using only information from the corresponding pre-shock period $\mathcal{T}_y^{\text{pre}}$.

Quadratic Pre-Trend Removal. To allow for nonlinear drift in connectivity, we estimate for each contract j:

$$Y_{jt} = \alpha_{j,y} + \beta_{1j,y}\tau_{t,y} + \beta_{2j,y}\tau_{t,y}^2 + \varepsilon_{jt}, \qquad t \in \mathcal{T}_y^{\text{pre}}, \tag{1}$$

where $\tau_{t,y}$ denotes a time index normalized to zero at the beginning of $\mathcal{T}_y^{\text{pre}}$. The detrended outcome is defined as

$$\tilde{Y}_{jt} = Y_{jt} - \hat{\beta}_{1j,y}\tau_{t,y} - \hat{\beta}_{2j,y}\tau_{t,y}^2. \tag{2}$$

Month-of-Year Residualization. To account for deterministic seasonality in network connectivity, we residualize Y_{jt} on month-of-year indicators:

$$Y_{jt} = \alpha_{j,y} + \sum_{m=1}^{12} \gamma_{jm,y}\mathbf{1}\{\text{month}(t) = m\} + \varepsilon_{jt}, \qquad t \in \mathcal{T}_y^{\text{pre}}. \tag{3}$$

The detrended outcome is then defined as the fitted residual

$$\tilde{Y}_{jt} = \hat{\varepsilon}_{jt}.$$

In all cases, detrending relies exclusively on pre-shock information to preserve the exogeneity of treatment assignment.

3 Empirical Results

3.1 Total communicability

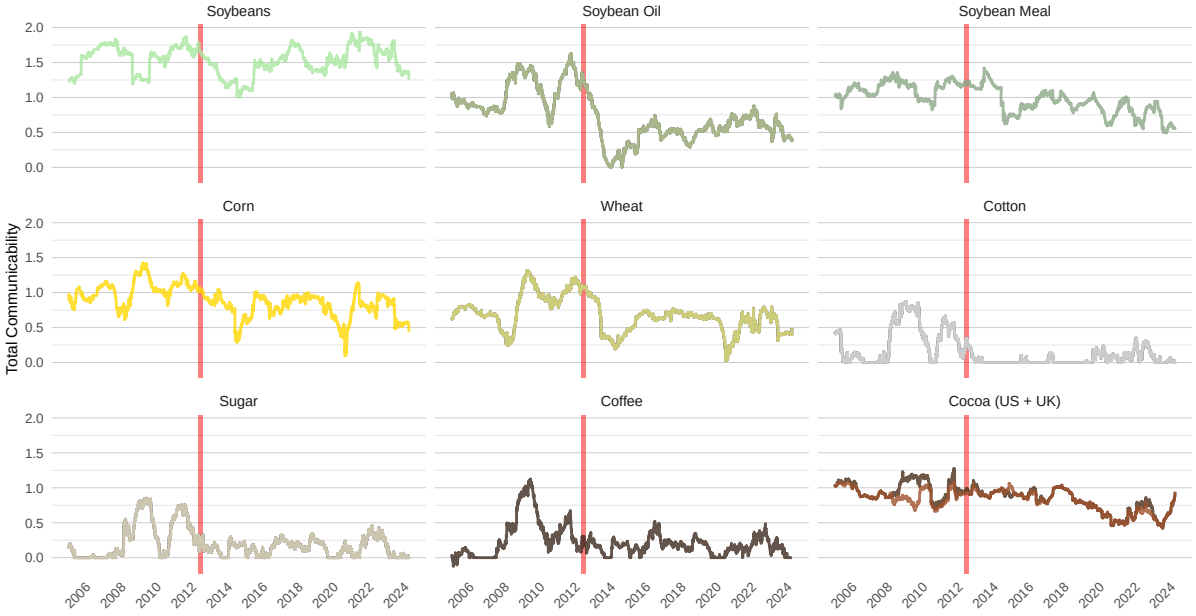


Figure 2. Total communicability of the contemporaneous graph. Red vertical line marks 2012 U.S. drought.



Figure 3. Total communicability of the directed Granger graph - shock transmission. Red vertical line marks 2012 U.S. drought.



Figure 4. Total communicability of the directed Granger graph - shock reception. Red vertical line marks 2012 U.S. drought.

3.2 Variation in Network Intensity

Date	I_t^C	ΔI_t^C	Z	p-value	Event
2008-09-12	1.7143	-0.2440	-20.85	0.0000	Lehman collapse
2021-07-15	1.7973	-0.1961	-16.75	0.0000	–
2013-07-15	1.9577	-0.1475	-12.60	0.0000	JPM exit
2010-07-16	2.2334	-0.1347	-11.51	0.0000	Russia grain export ban
2015-08-26	2.0076	-0.1171	-10.00	0.0000	–
2014-08-14	1.8970	-0.1168	-9.98	0.0000	Russia food import ban
2016-06-24	2.1128	-0.0794	-6.79	1.15e-11	Brexit
2008-09-15	1.6353	-0.0790	-6.75	1.51e-11	Lehman collapse
2020-09-16	1.7519	-0.0784	-6.70	2.12e-11	–
2014-07-14	2.0370	-0.0782	-6.68	2.42e-11	Russia food import ban
2022-03-15	1.9350	-0.0669	-5.71	1.11e-08	Russia–Ukraine war
2006-10-12	2.0118	-0.0654	-5.59	2.27e-08	–
2013-05-15	2.2188	-0.0641	-5.48	4.23e-08	–
2021-12-15	1.9487	-0.0617	-5.28	1.33e-07	–
2023-08-07	1.8102	-0.0613	-5.24	1.64e-07	–
2023-05-15	1.8699	-0.0595	-5.08	3.72e-07	–
2020-03-17	1.9780	-0.0588	-5.02	5.10e-07	WTI negative/ COVID shock
2022-09-16	1.9330	-0.0517	-4.42	9.90e-06	–
2023-08-14	1.7173	-0.0497	-4.25	2.14e-05	–
2005-07-14	2.1421	-0.0489	-4.18	2.92e-05	–

Table 4. Largest Negative Variations in Top-3 Contemporaneous Network Intensity. The table reports the largest negative daily changes in contemporaneous network intensity I_t^C obtained from rolling NETS estimations. For each 240-day rolling window, we estimate the contemporaneous partial correlation network using the NETS framework with fixed regularization parameters. Network intensity is defined as the sum of the three largest absolute contemporaneous partial correlations across all commodity pairs. The daily change ΔI_t^C measures the difference in intensity relative to the previous trading day. The standardized statistic Z is computed as the deviation of ΔI_t^C from its unconditional mean divided by its standard deviation over the full sample, and the reported p-value corresponds to a two-sided normal test. The table lists the twenty largest negative realizations of ΔI_t^C, which correspond to the sharpest contractions in contemporaneous cross-commodity dependence. The final column indicates major market or macroeconomic events occurring close to the reported dates.

Date	I_t^G	ΔI_t^G	Z	p-value	Event
2013-07-15	0.5139	0.5139	24.76	0.0000	JPM exit
2008-09-15	0.6410	0.3802	18.32	0.0000	Lehman collapse
2020-09-16	0.3358	0.2974	14.33	0.0000	–
2020-03-19	0.2600	0.2320	11.18	0.0000	WTI negative price
2014-08-14	0.3720	0.1855	8.94	0.0000	Russia grain/food import ban
2023-05-12	0.4020	0.1736	8.36	0.0000	–
2013-09-16	0.2928	0.1428	6.88	5.89e-12	–
2016-08-01	0.3134	0.1426	6.87	6.33e-12	–
2023-07-10	0.1819	0.1376	6.63	3.38e-11	–
2010-07-22	0.5123	0.1294	6.24	4.50e-10	Russia grain export ban
2010-02-12	0.2168	0.1161	5.60	2.18e-08	–
2010-02-17	0.3381	0.1159	5.59	2.33e-08	–
2023-02-23	0.3973	0.1136	5.47	4.41e-08	–
2010-08-04	0.6128	0.1007	4.85	1.21e-06	Russia grain export ban
2010-07-01	0.3629	0.0968	4.66	3.12e-06	Russia grain export ban
2023-04-28	0.4027	0.0943	4.54	5.56e-06	–
2023-04-27	0.3084	0.0926	4.46	8.12e-06	–
2020-03-27	0.3216	0.0925	4.46	8.28e-06	WTI turning negative
2011-03-21	0.2288	0.0902	4.35	1.37e-05	–
2016-07-27	0.1989	0.0894	4.31	1.65e-05	–

Table 5. Largest Positive Variations in Top-3 Predictive (Granger) Network Intensity. The table reports the twenty largest positive daily changes in predictive network intensity I_t^G obtained from rolling NETS estimations. Network intensity is defined as the sum of the three largest absolute Granger coefficients across directional commodity links. ΔI_t^G denotes the day-to-day change in this measure, Z is the standardized deviation relative to the unconditional distribution of ΔI_t^G, and the reported p-values correspond to two-sided normal tests. The final column indicates major events occurring near the reported dates.

Tables 4 and 5 document a pronounced asymmetry in extreme network variations. The largest negative realizations of ΔI_t^C (contemporaneous intensity) cluster around major financial and geopolitical announcements, including the Lehman Brothers collapse (2008), JPMorgan's exit from physical commodity trading (2013), and the Russian grain (2010) and food import (2014) bans. In contrast, the largest positive realizations of ΔI_t^G (predictive intensity) occur during the same episodes. This pattern is consistent with the mechanism proposed in the main text: fast shocks induce an immediate contraction of contemporaneous dependence (network fragmentation), while simultaneously generating sequential spillovers captured by the Granger network.

Event dates do not always coincide exactly with the formal announcement day. This is mechanically expected because network statistics are estimated using rolling 240-day windows, implying that structural breaks enter the estimates gradually as the window updates. In addition, anticipation, information leakage, and delayed market reactions may shift the peak statistical variation by several trading days. Therefore, the concentration of statistically extreme variations within a narrow window surrounding each event provides strong evidence of economically meaningful network reconfiguration rather than random fluctuation.

3.3 Drought sensitivity

	Cc1	Wc1	Sc1	SMc1	BOc1	SBc1	CTc1	KCCc1	CCc1	LCCc1
Corn		0.11	0.09	0.15	-0.02	-0.08	-0.12	-0.08	0.04	0.08
Wheat			0.14	0.16	0.14	-0.07	-0.07	0.01	-0.02	0.00
Soybeans				0.13	0.02	-0.06	-0.14	-0.02	0.10	0.14
Soybean Meal					0.15	-0.03	-0.10	0.02	0.13	0.16
Soybean Oil						-0.10	-0.06	-0.03	0.06	0.07
Sugar							0.06	0.07	0.01	0.02
Cotton								0.00	0.10	0.08
Coffee									0.00	-0.00
Cocoa US										0.05
Cocoa UK										

Table 6. The difference between the correlation matrix during the drought (May 2012–June 2013) and the correlation matrix over the whole period

We estimate the direct sensitivity of individual commodity returns to the 2012 U.S. drought using the following regression:

$$r_{i,t} = \alpha_i + \beta_i \cdot \text{Drought}_t + \varepsilon_{i,t},$$

where Drought_t is a dummy equal to 1 between 1 June 2012 and 1 September 2012, and $r_{i,t}$ denotes daily log returns. Results are reported in Table 7.

Table 7. Drought Sensitivity of Individual Commodity Returns

Commodity	**Drought Coefficient**	t**-Statistic**	p**-Value**
Corn (Cc1)	0.00508	2.16	0.0311
Soybean Meal (SMc1)	0.00462	1.92	0.0545
Wheat (Wc1)	0.00441	1.69	0.0917
Soybeans (Sc1)	0.00396	1.92	0.0545
Cocoa US (CCc1)	0.00263	1.13	0.2603
Soybean Oil (BOc1)	0.00201	1.01	0.3137
Cotton (CTc1)	0.00145	0.61	0.5417
Cocoa UK (LCCc1)	0.00125	0.60	0.5516
Sugar (SBc1)	−0.00016	−0.06	0.9492
Coffee (KCc1)	0.00008	0.03	0.9738

Several grains exhibit statistically significant shifts in returns. Drought-sensitive grains such as corn, soybean meal, soybeans, and wheat exhibit economically meaningful and statistically marginal-to-significant increases in return levels during the drought period. In contrast, softs such as coffee, cocoa, and sugar show no sensitivity as they are not directly affected by the US drought, and the shock propagation was not that strong.

3.4 Difference-in-Differences

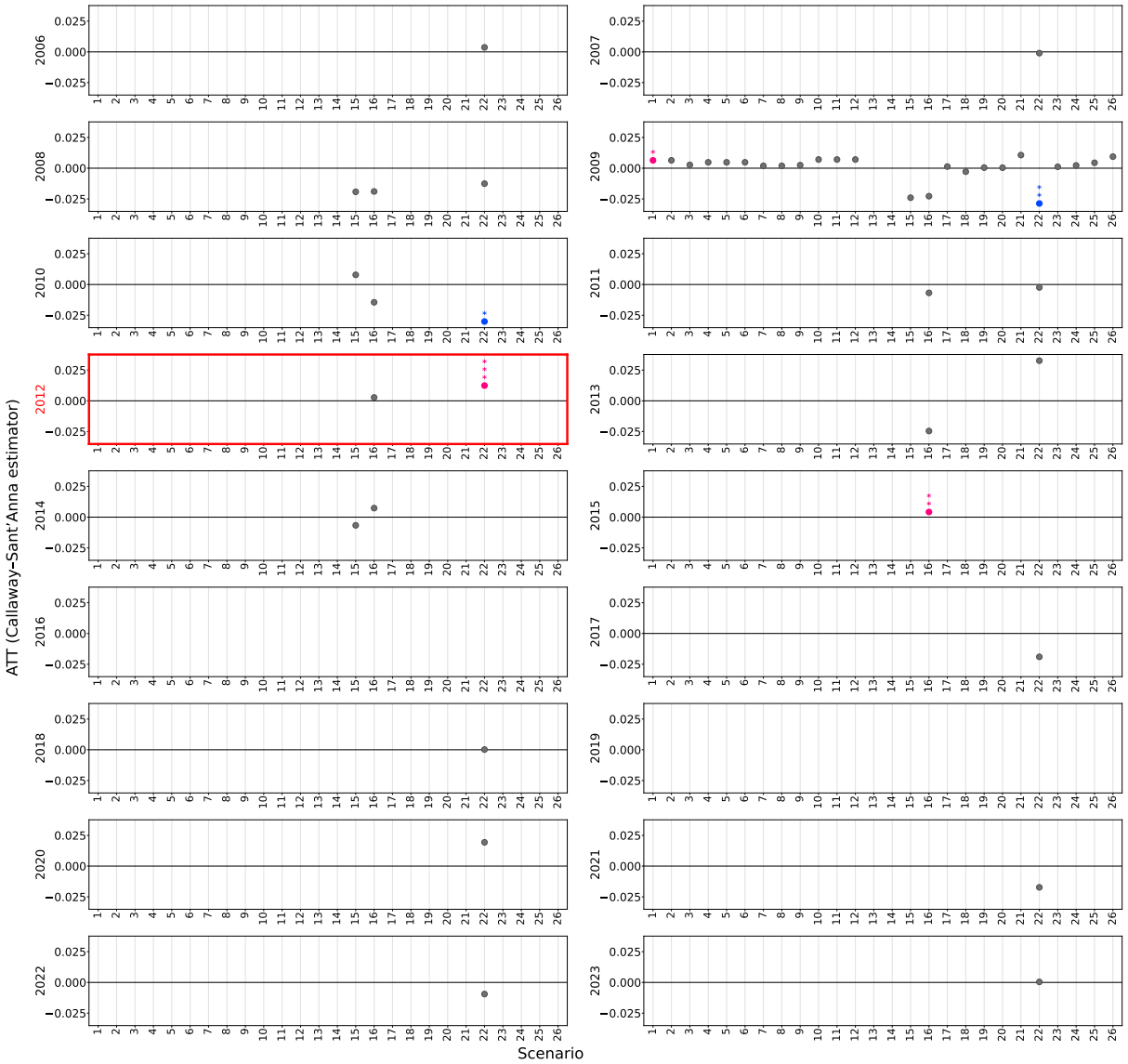


Figure 5. Corn and Wheat

Difference-in-differences estimates of drought impact on network Granger predictive connectivity: corn-wheat anchor basket, 2006-2023. Each panel displays ATT estimates for a given year across 21 robustness specifications (Table 5.2). Significance levels: * $p < 0.10$, ** $p < 0.05$, *** $p < 0.01$.

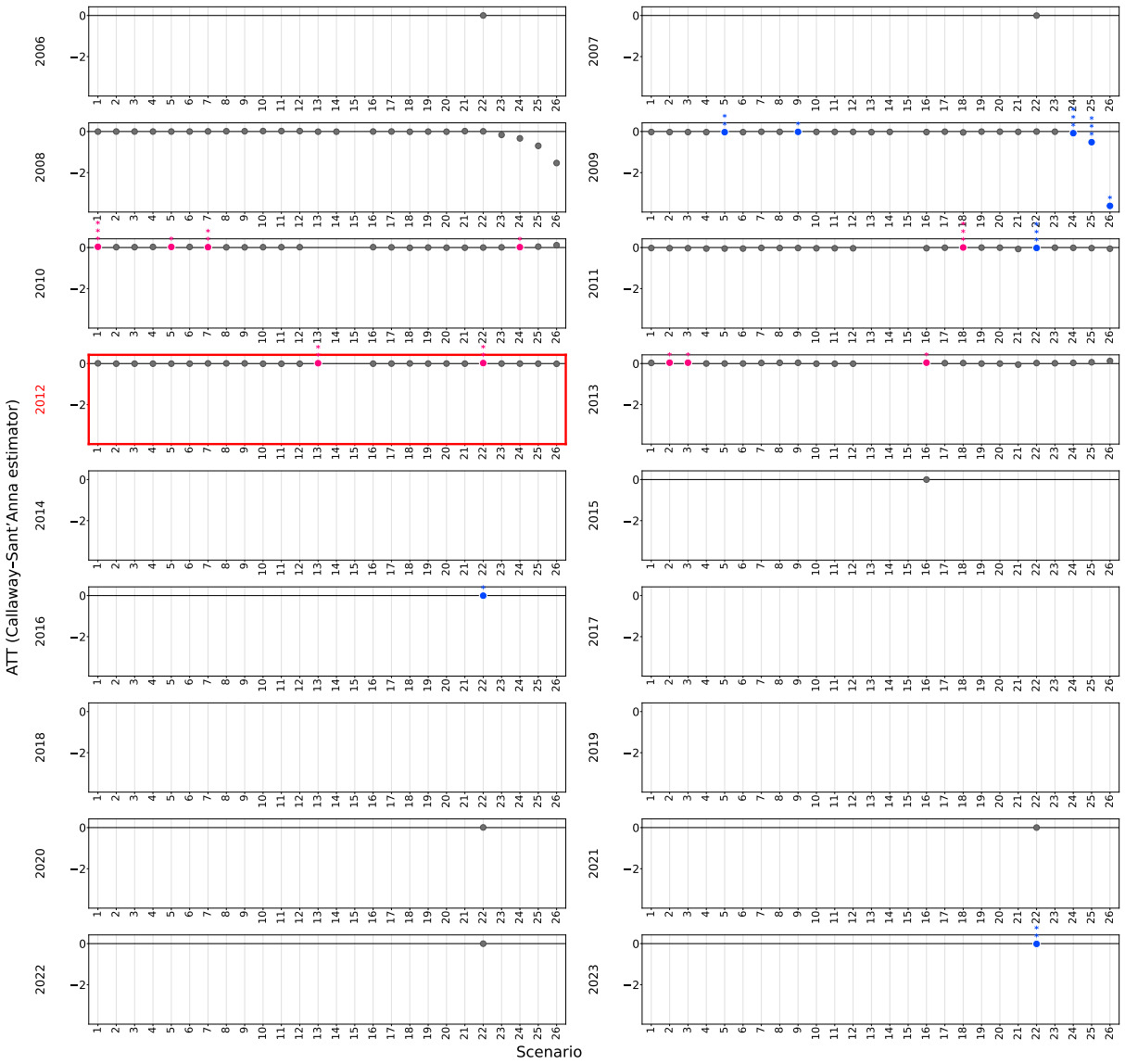


Figure 6. Soybeans, Soybean Oil and Soybean Meal

Difference-in-differences estimates of drought impact on network Granger predictive connectivity: corn-wheat anchor basket, 2006-2023. Each panel displays ATT estimates for a given year across 21 robustness specifications (Table 5.2). Significance levels: * $p < 0.10$, ** $p < 0.05$, *** $p < 0.01$.

For transparency, we complement the Callaway and Sant'Anna (2021) estimates with a calendar-time 2×2 DiD computed on the High–Low difference series, $D_t \equiv \bar{\bar{Y}}_{\text{High},t} - \bar{\bar{Y}}_{\text{Low},t}$ (Figure 7). Because this estimator collapses the post-shock window into a single indicator, it does not exploit event-time variation. Nevertheless, the estimates are consistently positive and often statistically significant in 2012, mirroring the sign and robustness of the Callaway–Sant'Anna $\text{ATT}^{\text{simple}}$ results. This concordance indicates that the 2012 drought is associated with a persistent widening in network exposure between High and Low contracts, rather than reflecting estimator-specific weighting or aggregation.

Outside 2012, the 2×2 DiD estimates are considerably less stable across specifications,

with frequent sign reversals and unstable significance.[1] This instability is not inconsistent with the Callaway–Sant'Anna results: when true effects are near zero, small differences in aggregation and variance estimation can generate apparent discrepancies across estimators. Accordingly, the calendar-time 2×2 DiD serves primarily as a diagnostic check in non-event years, while providing clear corroboration for the economically salient 2012 shock.

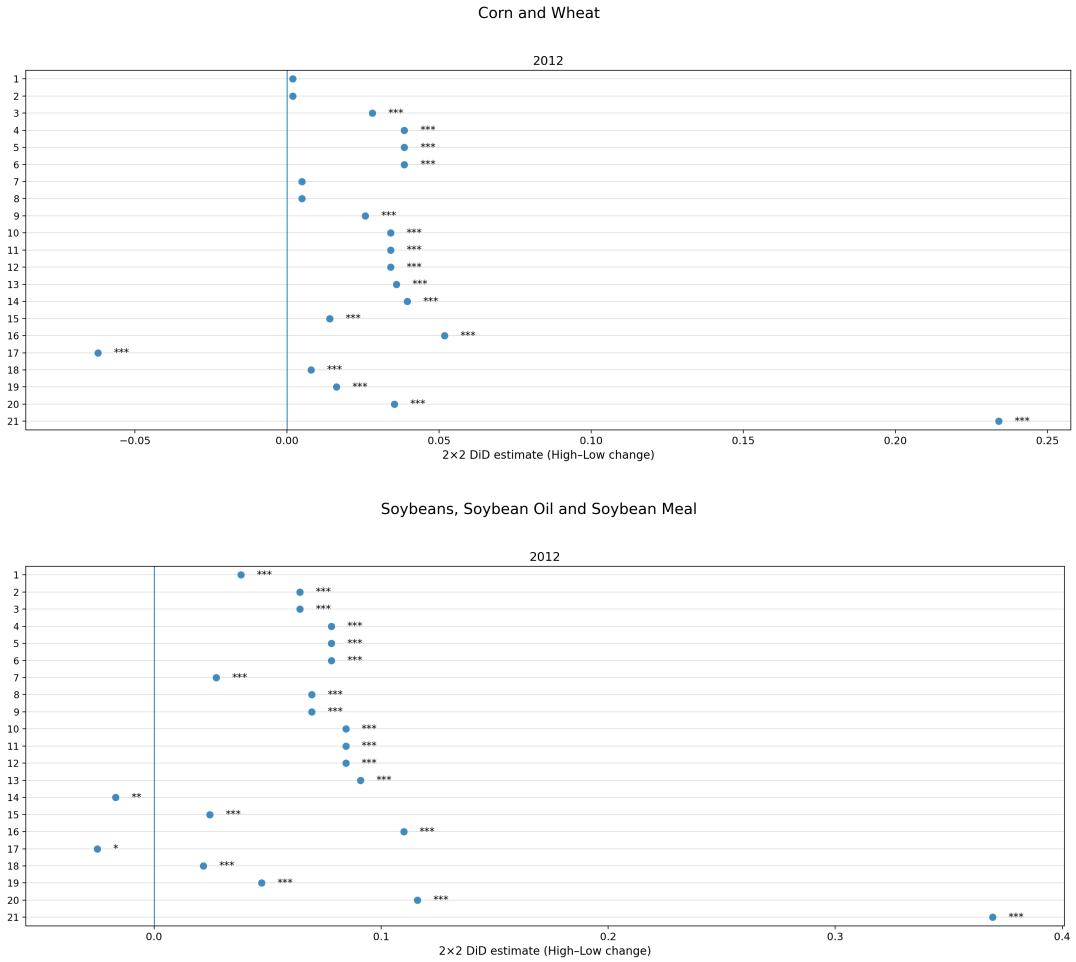


Figure 7. Calendar-time 2×2 DiD estimates for 2012 across specifications, shown separately by anchor basket (Corn-Wheat and Soybean-complex). We report simple DiD contrast computed on the High-Low difference in detrended network exposure. Inference uses Newey-West standard errors.

[1]Year-by-year 2×2 panels are omitted to avoid over-interpreting noise.